381
6-23-78

Ah. 202

FE-2030-9

FOSSIL ENERGY

# THE CHARACTERISTICS OF AMERICAN COALS IN RELATION TO THEIR CONVERSION INTO CLEAN ENERGY FUELS

Quarterly Technical Progress Report, July—September 1977

By
W. Spackman
A. Davis
P. L. Walker
H. L. Lovell
R. H. Essenhigh
F. J. Vastola
P. H. Given
N. H. Suhr

December 1977
Date Published

Work Performed Under Contract No. EX-76-C-01-2030

The Pennsylvania State University
Coal Research Section
University Park, Pennsylvania

MASTER

U. S. DEPARTMENT OF ENERGY

DISTRIBUTION OF THIS DOCUMENT IS UNLIMITED

## DISCLAIMER

This report was prepared as an account of work sponsored by an agency of the United States Government. Neither the United States Government nor any agency Thereof, nor any of their employees, makes any warranty, express or implied, or assumes any legal liability or responsibility for the accuracy, completeness, or usefulness of any information, apparatus, product, or process disclosed, or represents that its use would not infringe privately owned rights. Reference herein to any specific commercial product, process, or service by trade name, trademark, manufacturer, or otherwise does not necessarily constitute or imply its endorsement, recommendation, or favoring by the United States Government or any agency thereof. The views and opinions of authors expressed herein do not necessarily state or reflect those of the United States Government or any agency thereof.

**DISCLAIMER**

**Portions of this document may be illegible in electronic image products. Images are produced from the best available original document.**

## NOTICE

This report was prepared as an account of work sponsored by the United States Government. Neither the United States nor the United States Department of Energy, nor any of their employees, nor any of their contractors, subcontractors, or their employees, makes any warranty, express or implied, or assumes any legal liability or responsibility for the accuracy, completeness or usefulness of any information, apparatus, product or process disclosed, or represents that its use would not infringe privately owned rights.

This report has been reproduced directly from the best available copy.

Available from the National Technical Information Service, U. S. Department of Commerce, Springfield, Virginia 22161.

Price: Paper Copy $5.25
Microfiche $3.00

FE-2030-9
Distribution Categories UC-90a, 90b, 90c, 90d, 90e

# THE CHARACTERISTICS OF AMERICAN COALS IN RELATION TO THEIR CONVERSION INTO CLEAN ENERGY FUELS

## Quarterly Technical Progress Report
## July - September 1977

by
W. Spackman, A. Davis, P.L. Walker, H.L. Lovell,
R.H. Essenhigh, F.J. Vastola, P.H. Given and N.H. Suhr

COAL RESEARCH SECTION
THE PENNSYLVANIA STATE UNIVERSITY
UNIVERSITY PARK, PENNSYLVANIA 16802

DISTRIBUTION OF THIS DOCUMENT IS UNLIMITED

TABLE OF CONTENTS


| | Page |
|---|---|
| ABSTRACT | iii |
| OBJECTIVE AND SCOPE OF WORK | iv |
| TASK DESCRIPTIONS | v |
| SUMMARY OF PROGRESS TO DATE | 1 |
| SAMPLE COLLECTION AND SEAM CHARACTERIZATION | 4 |
| Sampling Survey | 4 |
| Sampling Plan | 4 |
| Coal Sampling | 4 |
| COAL CHARACTERIZATION | 5 |
| Coal Characterization | 5 |
| Rapid Scan Automated Reflectance Microscope System | 5 |
| SAMPLE BANK OPERATION, MAINTENANCE, AND DEVELOPMENT | 8 |
| Service to Other Agencies | 8 |
| PENN STATE/ERDA COAL DATA BASE | 9 |
| Interrelationships Among Chemical and Petrographic Variables of United States Coals | 9 |
| COAL BENEFICIATION AND PRE-USE PROCESSING | 22 |
| REACTOR DEVELOPMENT AND OPERATION | 23 |
| Characteristics of Chars Produced by Pyrolsis and Combustion Following Rapid Heating of Pulverized Coal | 23 |
| Evaluation of the Gasification Potential of Coals | 30 |
| COKES AND CHARS | 35 |
| Preoxidation of Caking Coals to Retard their Softening and Swelling | 35 |
| Methanol and Water Densities of Coals and Chars | 39 |
| Catalysis of Char Gasification | 41 |
| DIFFERENTIAL SCANNING CALORIMETRY | 46 |
| Chemisorption of Oxygen on Carbonaceous Solids | 46 |
| COMBUSTION OF CHARS AND LOW VOLATILE FUELS | 50 |
| Combustion of Char and Anthractie Coal in Large Utility Boilers | 50 |
| COMBUSTION OF COAL-OIL EMULSIONS | 55 |
| Combustion of Coal-Oil-Water-Air Mixtures | 55 |
| CONCLUSIONS | 60 |
| REFERENCES | 63 |
| CONTRIBUTORS | 64 |

## ABSTRACT

The Penn State/ERDA Coal Sample Bank was expanded to include 201 new coal samples (Facet I). A total of 68 characterized coal samples and 115 selected printouts of coal data were supplied upon request to the coal research community. Selected chemical and petrographic properties were statistically analyzed for 119 coal channel samples chosen from the Penn State/ERDA Coal Data Base.

Installation of the pressurized laminar flow isothermal reactor (Facet IV-A) has begun. Experiments have continued on the combustion pot; the study of the reactivity of a Koppers Company coke is now complete.

Studies under Facet IV-B show that weight changes associated with pre-oxidation can be precisely measured using a TGA apparatus. Water densities determined on 19 coals were lower when measured in the presence of a wetting agent. Study of the effect of reaction temperature on gasification of Saran carbon in air shows one percent platinum loading on Saran carbon increases gasification rates over the entire range of carbon burn-off.

The theoretical aspects of the study of combustion of low volatile fuels (Facet V-A) resumed. The computer model was expanded to include the effects of heat loss through the furnace walls, and its effect on flame temperature profiles.

Work on Facet V-B has led to minor furnace and control modifications, improvements in operating procedures, and an improved basis for evaluating experimental data toward accomplishment of the major objectives: investigation of the combustion characteristics of coal-oil-water-air fuel mixtures. Only through the use of non-equilibrium experiments can certain important combustion characteristics be studied, and computerized data acquisition is being developed to fully implement such methods.

## OBJECTIVE AND SCOPE OF WORK

The primary objective of the overall program is to achieve the capability of predicting, from a knowledge of coal composition, the behavior of a coal in pre-conversion processing, coal gasification and coal liquefaction processes.

It is reasonable to ask if this goal is in fact attainable, recognizing the heterogeneity of coal seams. Clearly, it is not if one concerns oneself simply with the rank of the coal seam and its aggregate chemistry. A high volatile B coal from Indiana need not react to processing in the same manner as a high volatile B coal from Utah, even though their "chemistries" may be very similar. In contrast, a coal lithotype of a specific kind, at a given level of rank, can be expected to behave consistently, whether it derives from Alabama or Pennsylvania. Hence, the goal may very well be attainable if, as in the case of coal carbonization, we concern ourselves with the reacting entities and the properties of the important lithotypes.

The goal is to attain the same high level of predictive accuracy that is now found in the area of coal carbonization, where Penn State's collaborative work with the steel industry proved highly successful. To achieve this goal Penn State has devised an integrated program in which the success of the research is highly dependent on the effective operation of ALL of the program's Facets and Sub-facets which are as follows:

Facet I: Characterization of the Nation's Coal Resources
- I-A: Sample Collection and Seam Characterization
- I-B: Coal Characterization
- I-C: Sample Bank Operation, Maintenance and Development
- I-D: Penn State-ERDA Coal Data Base

Facet II: Coal Beneficiation and Pre-Use Processing

Facet IV: Significance of Coal Characteristics in Gasification Processes
- IV-A: Reactor Development and Operation
- IV-B: Cokes and Chars
- IV-D: Reactivity of Coal Chars
- IV-E: Catalysis Research
- IV-F: Differential Scanning Calorimetry

Facet V: Coal Combustion Research
- V-A: Combustion of Chars and Low Volatile Fuels
- V-B: Combustion of Coal-Oil Emulsions

THE CHARACTERISTICS OF AMERICAN COALS IN RELATION TO THEIR CONVERSION INTO CLEAN ENERGY FUELS

## TASK DESCRIPTIONS

| | |
|---|---|
| FACET I-A | Sample Collection and Seam Characterization |
| Task 1 | Sampling Survey |
| Task 2 | Sampling Plan |
| Task 3 | Sampling |
| FACET I-B | Coal Characterization |
| Task 5 | Characteristics and Use Potential of U. S. Coal Seams |
| Task 6 | Characterization of Other ERDA Contractor Samples |
| Task 7 | Automation of Microscopic Analytical Methods |
| FACET I-C | Sample Bank Operation, Maintenance and Development |
| Task 8 | Maintenance of Coal Sample Bank |
| Tasks 9-14 | Provision of Samples and Data to Penn State and Other Investigators |
| FACET I-D | Penn State/ERDA Coal Data Base |
| Task 15 | Computerization of Data |
| Task 16 | Evaluation of the Data Base |
| Task 17 | Structuring and Utilization of the Data Base |
| FACET II | Coal Beneficiation and Pre-Use Processing |
| Task 18 | Washability Characterization |
| Task 19 | Physical Properties of Coal Lithotypes |
| Task 20 | Techniques for Fractionation |
| Task 21 | Beneficiation of Conversion Feedstocks |
| Task 22 | Evaluation of Dry Flo Separator |
| FACET IV-A | Reactor Development and Operation |
| Task 23 | Operation of Isothermal Furnace |
| Task 24 | Pyrolysis of Coal Lithotypes |
| Task 25 | Operation of Pressurized Isothermal Reactor |
| Task 26 | Coal Reactivity |
| FACET IV-B | Cokes and Chars |
| Task 27 | Effect of Variables on Char Structures |
| Task 28 | Effect of Char Structures on Reactivities |
| Task 29 | Catalytic Effect of Minerals in Gasification |
| Task 30 | Effect of Catalytic Cations on Gasification |
| FACET IV-F | Differential Scanning Calorimetry |
| Task 31 | DSC in Evaluating Coals for Conversion |
| FACET V-A | Combustion of Chars and Low Volatile Fuels |
| Task 32 | Flame Ball Combustion Model |
| Task 33 | Plane Flame Furnace |
| FACET V-B | Combustion of Coal - Oil Emulsions |
| Task 34 | Combustion of Coal - Oil Emulsions |

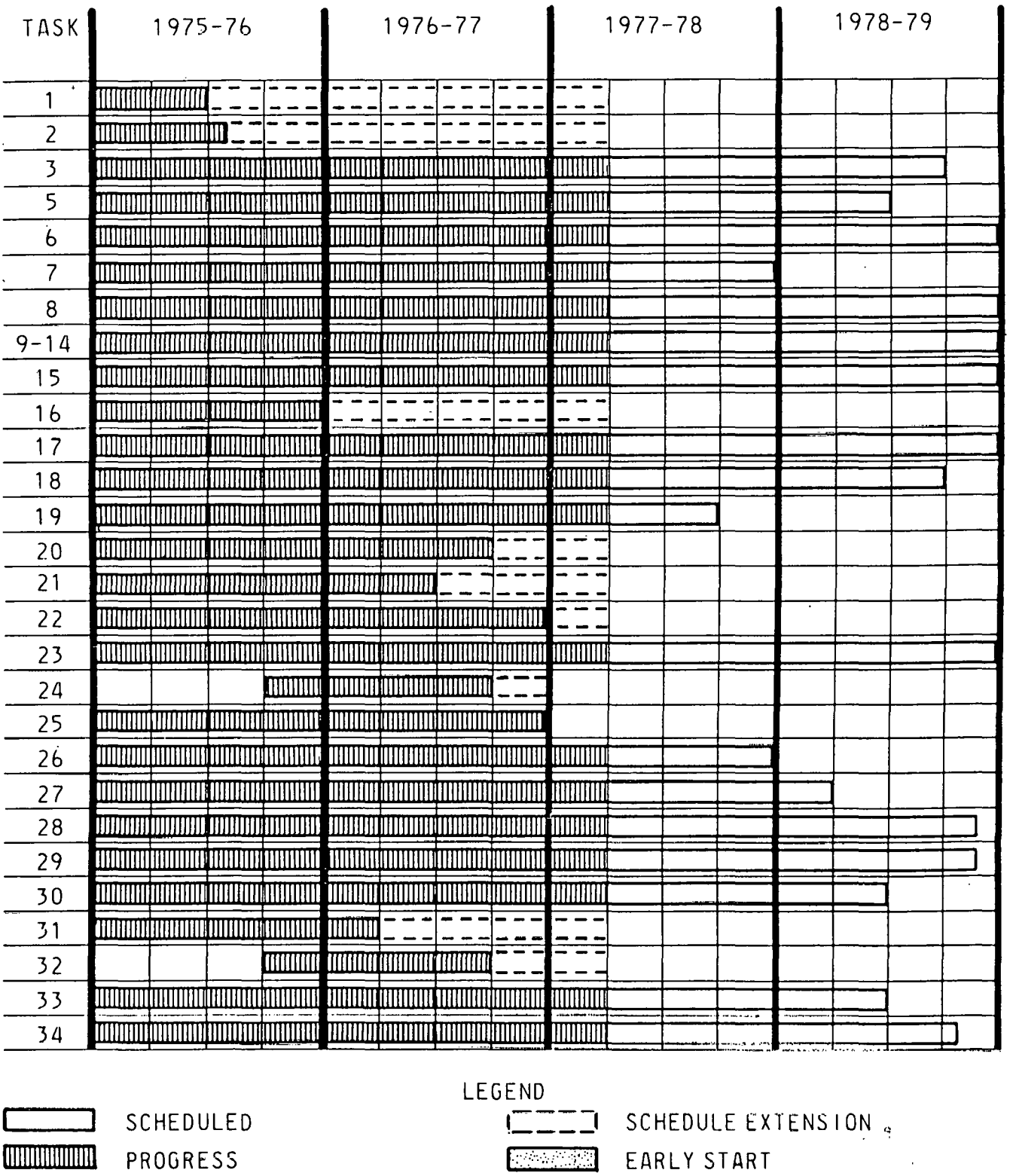


**PROJECT PLAN AND PROGRESS REPORT**
**Quarter Ending September 30, 1977**

## SUMMARY OF PROGRESS TO DATE

Under Facet I Penn State personnel collected 80 new coal samples this quarter. An additional 121 coal samples were collected for our program by subcontracted agencies. To date the sample bank contains 906 coal samples. A total of 68 characterized samples and 115 selected printouts of coal data were supplied to other agencies engaged in coal research. Reports concerning our sampling plan and our nationwide survey, conducted to determine the extent to which the Nation's coals have been characterized, are in the final stages of preparation.

Work under Task 7 (automated reflectance microscope system) has centered on the development of a computerized technique which will enable a quantitative analysis of reflectogram data.

One hundred and nineteen coal channel samples, chosen from the Penn State/ERDA coal data base, have been statistically analyzed with respect to selected chemical and petrographic coal properties (Task 17). Interrelationships between these properties were determined through factor and cluster analyses. An interim report of these findings is in preparation.

A pressured laminar flow isothermal reactor (Facet IV-A) has been designed, constructed and delivered to the Combustion Laboratory by Autoclave Engineers, Inc. The design of a hydrogen-safe building is complete, but because the availability of the building is not expected for at least one year, the reactor is being installed in the Combustion Laboratory, where important initial experiments will be carried out.

During this quarter 15 experiments were conducted to evaluate the reactivity of a Koppers Company coke. To date, a total of 52 combustion pot experiments have been conducted, with an emphasis on the effect of fuel type and fuel size on gasification rate. The consistent measure of activation energy of the $C/CO_2$ reaction in the gasification region at about 50 kcal for each coke provides an important datum in the development of the numerical model, and for the continuing evaluation of gasification potential of coals.

Under Facet IV-B a series of 13 samples were prepared from a lignite char by (1) depositing different amounts of carbon by the cracking of methane, and (2) activation of the raw and carbon deposited samples to different levels of carbon burn-off. Methanol and water densities of various samples were found to be very close to the helium densities. Water densities, determined on 17 coals varying in rank from low volatile bituminous to lignite, were found to be invariably higher than the corresponding helium densities.

Coals of certain rank (high volatile B to low volatile bituminous) soften and become plastic upon heating (350-500°C). These plastic coal particles agglomerate and, as gases and vapors are evolved, swell to form cokes, a phenomenon essential for the production of metallurgical cokes. However,

the same softening properties can make some coals impractical for direct use in gasifiers and some combustion units because these agglomerates impede air flow, leading to poor mixing in reactors and eventual plugging. The most common method of removing caking behavior is preoxidation of the raw coal at temperatures in the range 150-200°C. Although this method is very effective in removing softening properties, it reduces the calorific value of the coals and involves an extra processing step which is costly and reduces overall thermal efficiency. In addition, very little is known about the effect of preoxidation on the reactivity of coals toward gasification. This study attempts to quantify the effects of preoxidation on the caking properties of certain coals and to determine the effect of this pretreatment on the reactivity of these coals and their corresponding chars in gasification reactions.

As discussed previously, preparations have been made to examine the utility of a Dupont 942 Thermomechanical Analyzer (TMA) as a method of characterizing the swelling behavior of coals. This instrument measures vertical displacement of a dilatrometric probe which rests on top of a powdered sample. Hopefully, this will produce a quantitative method for determining the amount of swelling which occurs under carefully monitored heating conditions. This method will be used to follow the effects on swelling of such variables as particle size (35x60 mesh, 100x150 mesh and 200x250 mesh) and heating rate (10°C/min to 50°C/min). Unfortunately, this facet of the investigation has been delayed because the Dupont 990 thermal analyzer, which controls the 942 TMA, needed to be repaired. The unit will be available shortly, at which time the study will be resumed.

Under Task 29, work has been initiated to study the reactivity in air of Saran carbon as a function of platinum loading and its degree of dispersion.

Differential scanning calorimetry (Facet IV-F) has been established as a fast experimental technique for characterization of carbonaceous materials. The effect of different variables such as the level of carbon burn-off, particle size, bed height of carbon, reaction temperature, and flow rate on the heat of oxygen chemisorption on Saran carbon has been examined at 281°C. Below 100°C, the chemisorption process is associated with a significant physical absorption process, whereas above 125°C significant gasification also occurs. The active surface area accessible to oxygen during chemisorption at 100°C, determined mass spectrometrically, is 52 $m^2/g$ carbon. Increase in desorption soak time at 600°C prior to oxygen chemisorption at 100°C decreases both the heat released during chemisorption as well as the amount of oxygen chemisorbed. However, the magnitude of $\Delta H$ (kcal/mole) is independent of soak time. Increase in desorption temperature in the range 450-700°C, used to clean the carbon surface prior to chemisorption, increases the subsequent value of Q measured at 100°C. Increase in the heating rate from 1 to 10°C/min during heat pretreatment up to 600°C increases the subsequent value of Q at 100°C. However, this Q is independent of heating rates greater than 10°C/min.

Computer models are being improved and expanded continuously to study the combustion of pulverized char flames under Facet V-A. Assuming an infinite parallel plane geometry (properties vary only along the direction of flow) as a starting point toward further three-dimensional modeling, the results are compared with the experimental results obtained for four coal chars which have been burned in a plane-flame furnace at common air flow rates. Modifications to the model such as uneven nodal spacing, variable radiation absorption coefficients, and diffusional limitations on combustion rates have brought the results of the model closer to reality. The effect of varying parameters such as combustion length (between walls) and fuel reactivity has been investigated. A study was performed to compare the operations of the plane flame furnace with a hot refractory bottom and with a water-cooled metal bottom in order to assess the significance of end wall radiation on the flame characteristics. Most recently, the model has been expanded to include the important consideration of the loss of heat through the furnace walls.

Most of the specified objectives for Facet V-B have been probed preliminarily. Coal, oil, water, and air have been mixed in a number of ratios to establish the general behavior of the mixtures, and of the experimental equipment. A recent digression to characterize the furnace and its dynamic responses has laid the foundations for a more complete and systematic evaluation of the ranges of mixtures prescribed in the work statement.

## FACET I-A: SAMPLE COLLECTION AND SEAM CHARACTERIZATION

### SAMPLING SURVEY (TASK 1)

A nationwide survey to determine the extent to which the Nation's coals have been sampled and characterized is complete. An interim report of these findings is in the final stages of preparation.

### SAMPLING PLAN (TASK 2)

A coal sampling plan is in the final stages of preparation.

### COAL SAMPLING (TASK 3)

During July of this quarter a sampling trip was made to Ohio where thirty-one channel and lithotype samples were collected (PSOC-748 through 766, and PSOC-770 through 781) in six different counties. In August a sampling trip was made to three western states. Two large channel samples and seven lithotype samples (PSOC-833 through 841) were collected in Montana, two large channel samples and six lithotypes were collected in Wyoming (PSOC-842 through 849) while four large channel samples and 13 lithotypes were collected in Colorado (PSOC-850 through 866). Also during August a brief trip was made to Eastern and Northeastern Pennsylvania where channel samples of four anthracite seams were obtained along with three lithotype samples and a run-of-mine sample (PSOC-867 through 874), and in Lycoming County, three channel samples of low volatile bituminous coal were collected along with five lithotype samples (PSOC-875 through 882).

Our sampling subcontract with Texas A & M produced sixty-seven samples during this period. These were coal samples from Arkansas, Oklahoma, Texas, and New Mexico. Forty-four samples of West Virginia coals were received as a result of our contract with West Virginia University and six samples of Illinois coals were received from Southern Illinois University. In addition, we received four samples of Missouri coal from the Missouri Department of Natural Resources.

## COAL CHARACTERIZATION (TASK 5)

Maceral and reflectance analyses were completed on 36 PSOC coals along with two fluorescence analyses. Maceral analyses were also completed on 33 washability fractions from PSOC-324. The free-swelling index and Hardgrove grindability were determined for 63 coals. In addition, Gray-King coke types were determined for 4 of these same coals.

The Penn State Mineral Constitution Laboratories provide elemental and mineralogical data on PSOC coal samples. Most of the major, minor, and trace element data are being obtained from high temperature coal ashes (750°C). A plasma emission spectrometer is being used to determine the elements aluminum, barium, beryllium, calcium, copper, iron, potassium, magnesium, strontium, manganese, sodium, silicon, titanium, vanadium, zinc, and zirconium, while a d.c. arc spectrograph is employed for the determination of silver, bismuth, cerium, cobalt, chromium, gallium, lanthanum, molybdenum, niobium, lead, scandium, tin, yttrium, and ytterbium. In addition, rubidium and mercury are being determined by atomic absorption spectroscopy on the high temperature ash and as-received coal respectively while uranium is determined by the neutron activation analysis of the as-received coal. Mineralogical analyses are being obtained from low temperature coal ashes using x-ray diffraction (for calcite, pyrite and quartz) and I.R. (for kaolinite and gypsum) techniques. Qualitative x-ray diffraction and infra red patterns are also taken of each sample to determine the presence of phases not determined quantitatively. The amounts of these phases (for example, illite, montmorillonite, iron sulfates) are then estimated using available chemical data. The number of samples processed to date can be summarized as follows:

| | |
|---|---|
| PSOC coal received | 550 |
| High temperature ashes obtained | 490 |
| Low temperature ashes obtained | 265 |
| Major and minor element analyses | 180 |
| Trace element analyses | 176 |
| Mineralogical analyses | 100 |
| Mercury determinations | 221 |
| Uranium determinations | 239 |
| Moisture determinations | 238 |

A flow diagram of the entire analytical procedure is presented in Figure 1.

## RAPID SCAN AUTOMATED REFLECTANCE MICROSCOPE SYSTEM (TASK 7)

Work under Task 7 has involved the development of a computerized modeling technique which will enable a quantitative analysis of reflectogram data. This model attempts to generate petrographic and vitrinite reflectance information directly from a Rapid Scan reflectogram. A suite of coals of varying petrographic makeup have been analyzed to test the model. For

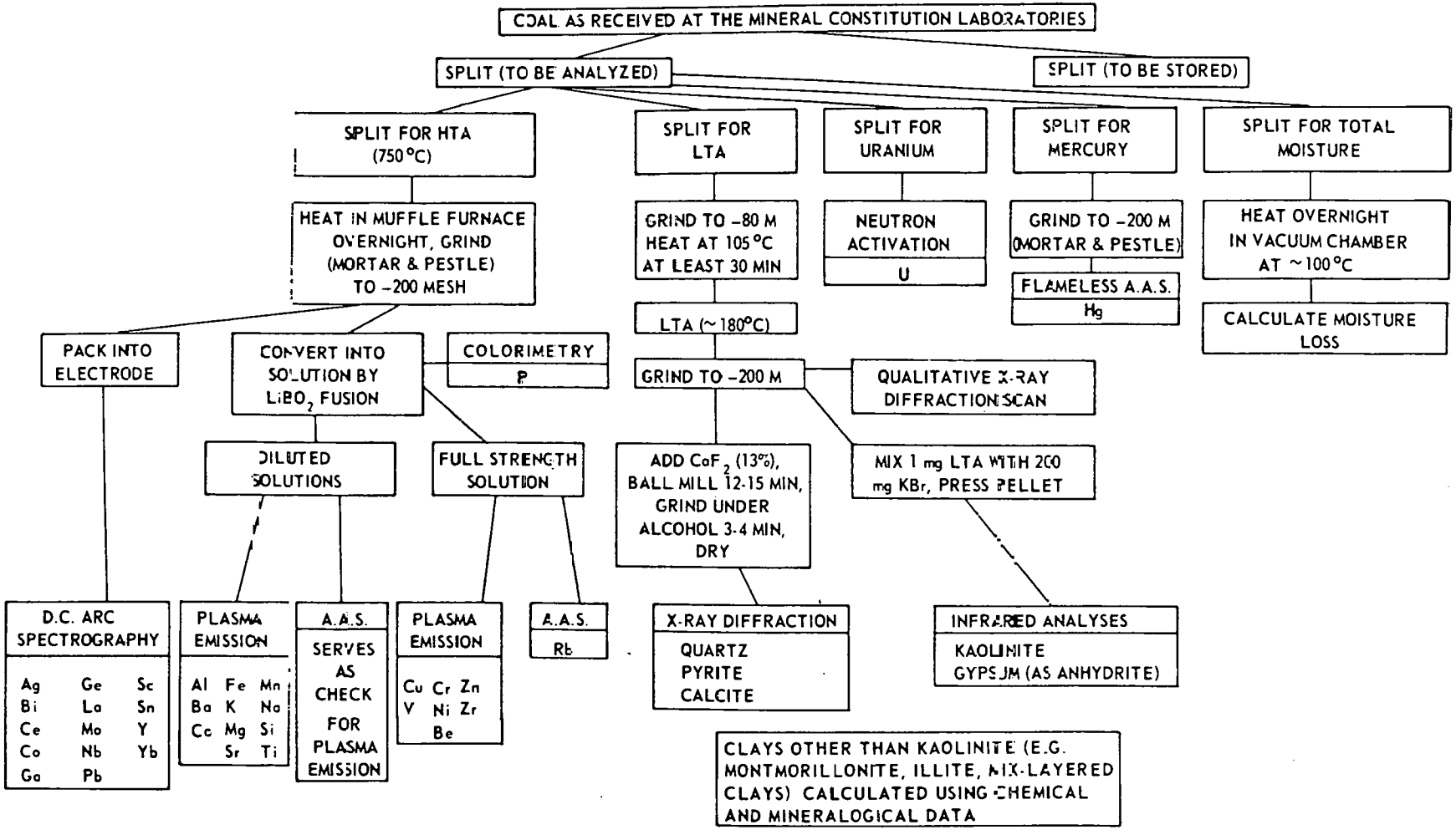


Figure 1. ANALYTICAL SCHEME FOR PSOC COALS AT THE PENN STATE MINERAL CONSTITUTION LABORATORIES

coals of greater than 70 percent vitrinite the technique has been quite successful in duplicating conventional analyses (see Figure 1). However, for coals of lower than 70 percent vitrinite the correlation has been less successful. This problem is related directly to the limited resolution of the current Rapid Scan system. Some improvements in resolution should be possible when new computer facilities become available. However, a digital scanning stage will be necessary before accurate petrographic analyses of coals with low vitrinite contents can be accomplished with an automated reflectance microscope.

Future work will involve continued pyrite analysis, improvements to the petrographic modeling programs, and the implementation of new computer facilities.

FACET I-C: SAMPLE BANK OPERATION, MAINTENANCE AND DEVELOPMENT

SERVICE TO OTHER AGENCIES (TASKS 8-14)

A total of 68 characterized coal samples and 115 selected printouts of coal data were supplied, at their request, to other agencies engaged in coal research (Tasks 8-14).

The agencies requesting these materials (and their research interest) include: City College of New York, Department of Chemical Engineering (char studies); General Electric Space Technology Center (sulfur studies); The Institute of Gas Technology (gasification kinetics); Air Products and Chemical Company (sulfur removal); Florida Atlantic University, Department of Chemistry (geochemical study); General Electric Research and Development (sulfur study); Kentucky Center for Energy Research (fluidized bed combustion); Portland State University (porosity and surface area study); Jet Propulsion Laboratory, California Institute of Technology (desulfurization studies); University of New Hampshire (catalytic liquefaction); West Virginia University, Department of Geology and Geography (comparative coalification study); and the Worcester Polytechnical Institute, Chemistry Department.

## FACET I-D: PENN STATE/ERDA COAL DATA BASE

### INTERRELATIONSHIPS AMONG CHEMICAL AND PETROGRAPHIC VARIABLES OF UNITED STATES COALS (TASK 17)

One hundred and nineteen coal channel samples (Figure 2), selected from the Penn State/ERDA Coal Data Base, have been statistically analyzed with respect to the coal properties listed in Table 1. A series of packaged, statistical, computer programs available through The Pennsylvania State University Computation Center were implemented in completing this study. These programs and their applications appear in Table 2.

A factor analysis of these data (Table 3) indicates that 45 percent of the variation within the data set is correlated with changes in coal rank. Variables which vary with rank include carbon, oxygen, calorific value, moisture, volatile matter, and reflectance. Maceral composition accounts for the next greatest source of variation. Hydrogen content was recognized by the analysis as virtually rank independent. This result is attributable to the curvilinear response of hydrogen to increasing rank (Figure 3). Nitrogen and sulfur each are independent of all other variables.

Although a cluster analysis indicates that the data set represents a continuum, the samples can be dissected into four groups distinguished on the basis of coal rank, relative maceral composition, and organic sulfur content (Figure 4). Factor analyses of the individual groups provide insights into the various stages of coalification. Carbon, oxygen, and calorific value vary together and are strongly affected by coalification for most rank levels. Reflectance, moisture, and volatile matter usually vary together except at high rank. Hydrogen content increases with rank until the middle levels of high volatile bituminous rank, and then decreases. It is at rank levels of medium volatile bituminous and higher where a distinct change is observed in the response of the variables to coalification: reflectance, volatile matter, and hydrogen are strongly correlated with rank, while carbon, oxygen, and calorific value no longer correlate strongly with rank, and behave independently of each other.

In the future, these four sample groupings, determined by cluster analysis, may be useful in the selection of representative coal types for the study of coal behavior during industrial use. As more samples become available these groups will be further tested.

Coal samples were also grouped and studied according to geographic origin (coal province). Factor analyses of coals from the Eastern, Rocky Mountain, and Northern Great Plains Provinces show that coal properties are consistent with coal rank. In contrast, Interior Province coals, intermediate in rank and highest in organic sulfur content, have unusually high moisture contents and low reflectance values for their given rank levels.

Bivariate plots of selected coal properties allow visual appreciation of relationships which exist between the coal characteristics discussed. Included for study are plots of vitrinite reflectance versus carbon content

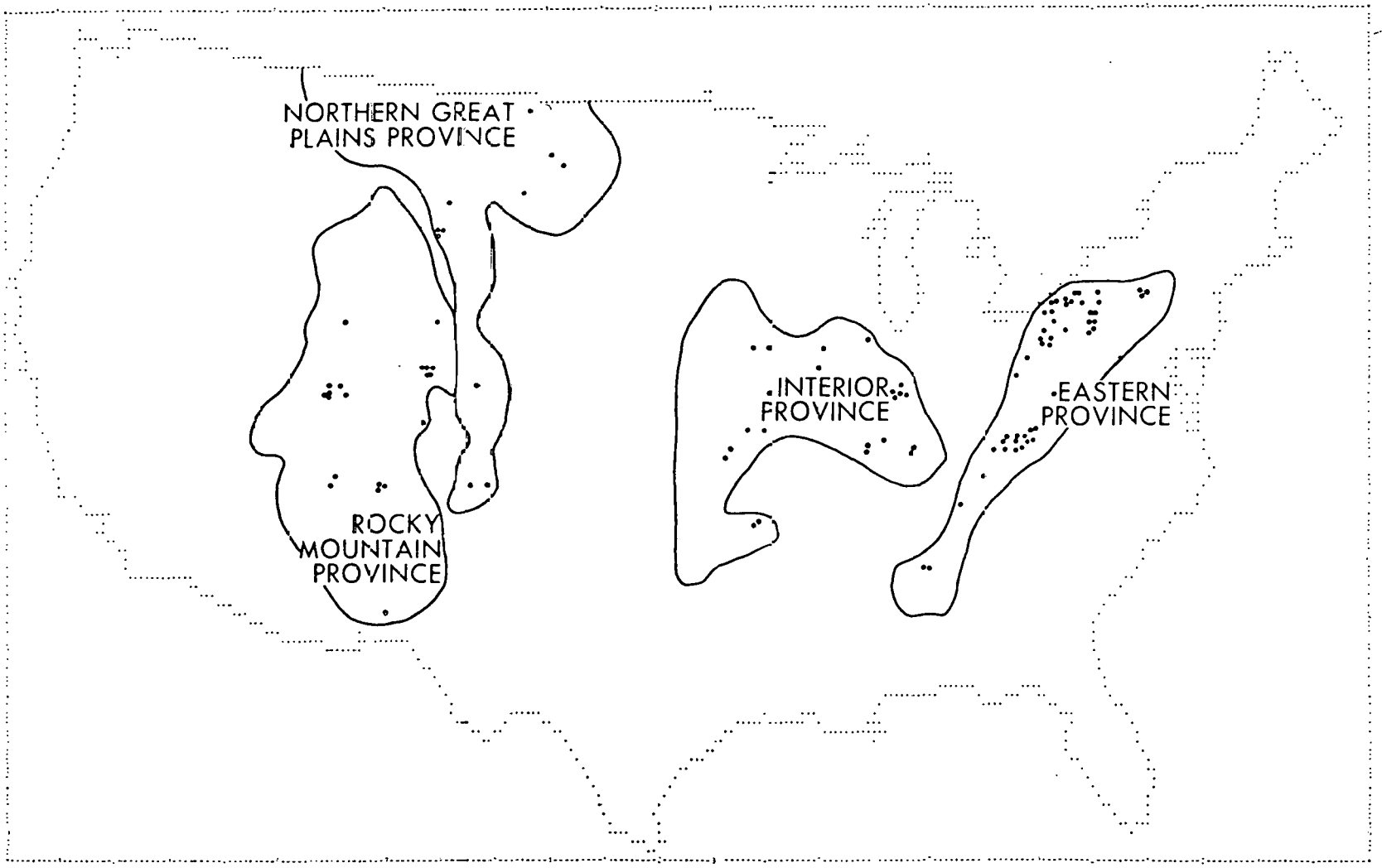


Figure 2. LOCATIONS OF PROVINCES AND SAMPLING SITES

Table 1. Coal Properties Studied

| Chemical | Petrographic |
|---|---|
| % Carbon | % Maximum Reflectance |
| % Hydrogen | % Vitrinite |
| % Organic Sulfur | % Liptinite |
| % Nitrogen | % Inertinite |
| % Oxygen | |
| % Moisture | |
| % Volatile Matter | |
| Calorific Value | |

Table 2. Statistical Techniques

| Statistical Technique | Program |
|---|---|
| Univariate Analysis<br>Test of frequency distributions for normality | NORMSTAT |
| Factor Analysis<br>Test of interactions between variables | CORFAN |
| Cluster Analysis<br>Procedure for classifying samples | CLUS |
| Bivariate plots of rank | STPAC |

Table 3. Original Matrix of Factor Loadings of the R-Mode Component Analysis of United States Coals

| | F 1 | F 2 | F 3 | F 4 | F 5 | F 6 | $h_i^2$ |
|---|---|---|---|---|---|---|---|
| Reflectance, % in oil | -0.95029 | -0.04875 | 0.00414 | 0.15384 | 0.04373 | -0.01767 | 0.93134 |
| Carbon, % dmmf | -0.95300 | -0.00073 | -0.19495 | 0.00576 | -0.07225 | 0.01498 | 0.95169 |
| Hydrogen, % dmmf | 0.33536 | 0.38679 | -0.71891 | 0.16440 | 0.11194 | -0.39488 | 0.97439 |
| Oxygen, % dmmf | 0.94717 | 0.10334 | 0.16612 | 0.09632 | 0.04767 | -0.06864 | 0.95166 |
| Sulfur, % dmmf | 0.08017 | 0.02000 | -0.42792 | -0.73270 | -0.49548 | 0.09872 | 0.98203 |
| Nitrogen, % dmmf | -0.15234 | 0.08546 | -0.37464 | -0.33116 | 0.81537 | 0.22762 | 0.99717 |
| Volatile matter, % dmmf | 0.87628 | 0.27234 | -0.28205 | -0.09923 | -0.02029 | -0.09410 | 0.94070 |
| Moisture, % mmf | 0.87967 | -0.17068 | 0.17064 | -0.10140 | 0.04298 | 0.19843 | 0.88358 |
| Btu/lb, % dmmf | -0.93252 | 0.05946 | -0.26969 | -0.00517 | -0.09677 | -0.02816 | 0.95695 |
| Vitrinite, vol. % mmf | 0.23889 | -0.90639 | -0.32063 | 0.06946 | 0.02013 | -0.05891 | 0.99012 |
| Inertinite, vol. % mmf | -0.29576 | 0.60525 | 0.55576 | -0.40182 | 0.12433 | -0.23335 | 0.99494 |
| Liptinite, vol. % mmf | 0.12945 | 0.76685 | -0.26535 | 0.38222 | -0.18818 | 0.37370 | 0.99638 |
| Sum $\lambda_i^2$ | 5.42306 | 2.05314 | 1.56940 | 1.03905 | 0.99516 | 0.46933 | |
| % Variation explained | 45.19217 | 17.10947 | 13.07833 | 8.65875 | 8.29301 | 3.91111 | |
| Cumulative % | 45.19217 | 62.30164 | 75.37997 | 84.03870 | 92.33170 | 96.24280 | |

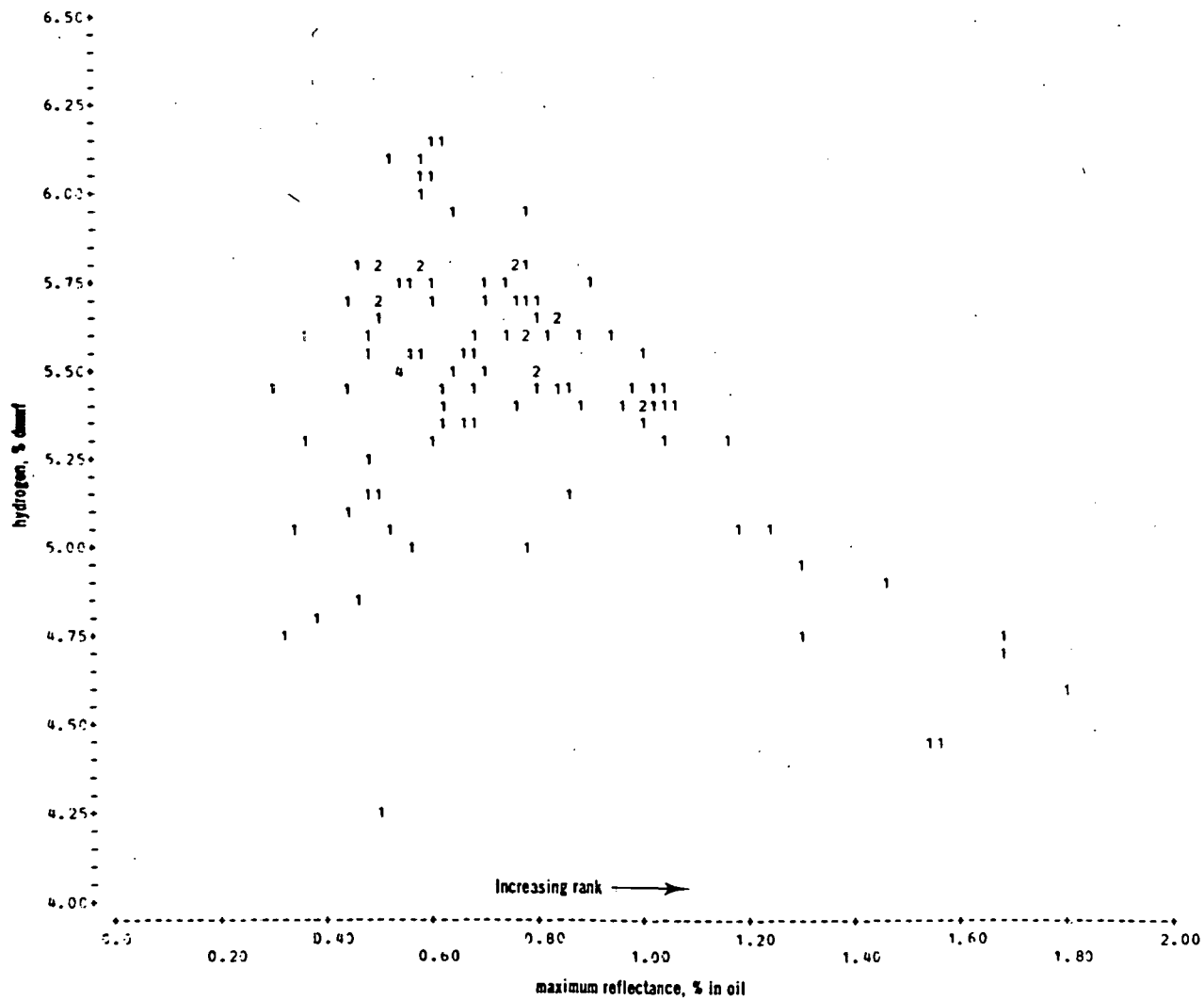


Figure 3. CURVILINEAR RESPONSE OF HYDROGEN TO INCREASES IN RANK

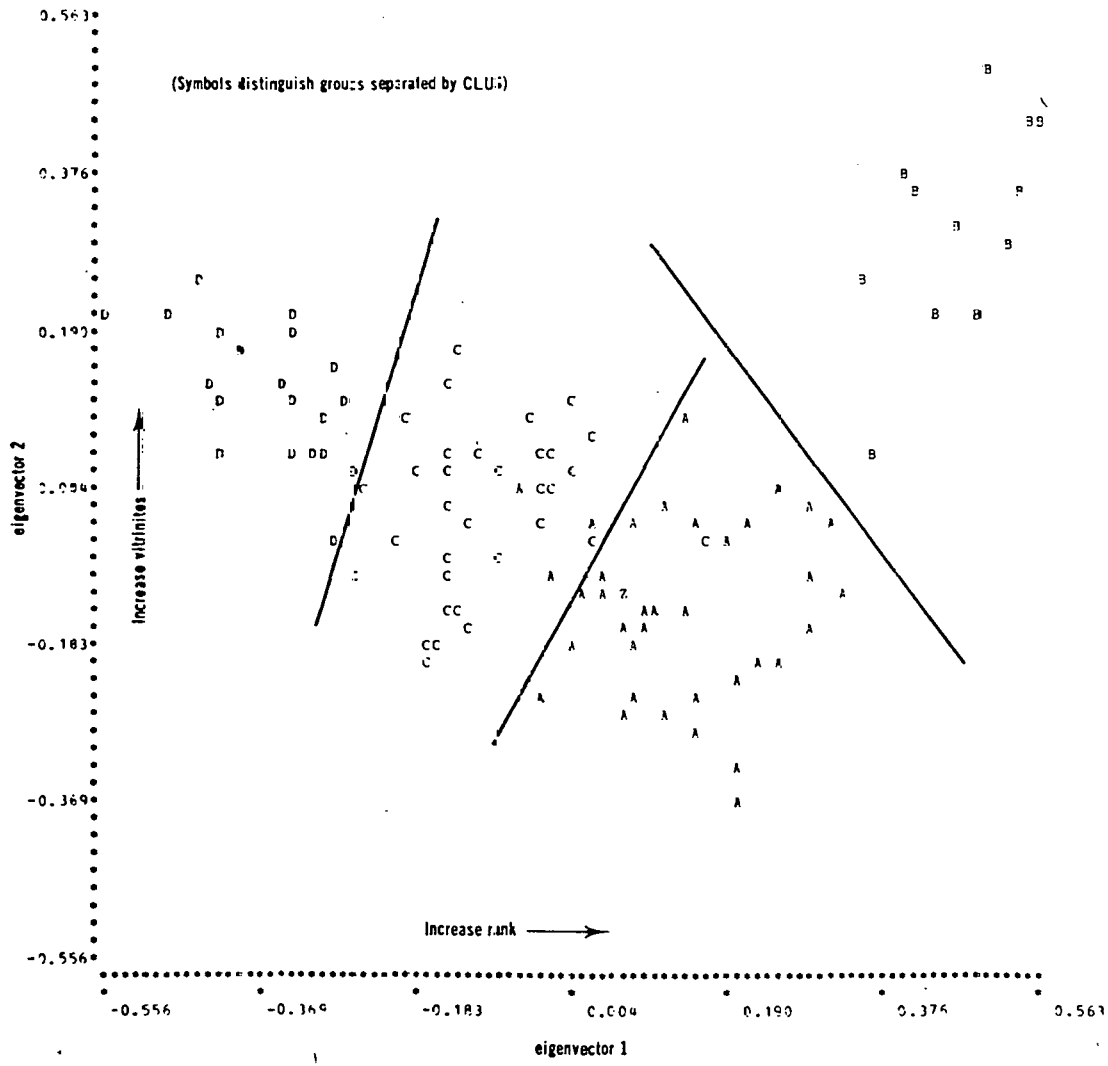


Figure 4. PLOT OF CLUSTER ANALYSIS OF U.S. COALS WHEN FOUR GROUPS ARE REQUESTED

(Figure 5), vitrinite reflectance versus calorific value (Figure 6), vitrinite reflectance versus liptinite maceral content (Figure 7), vitrinite reflectance versus moisture content (Figure 8), carbon versus oxygen content (Figure 9), and carbon versus moisture content (Figure 10).

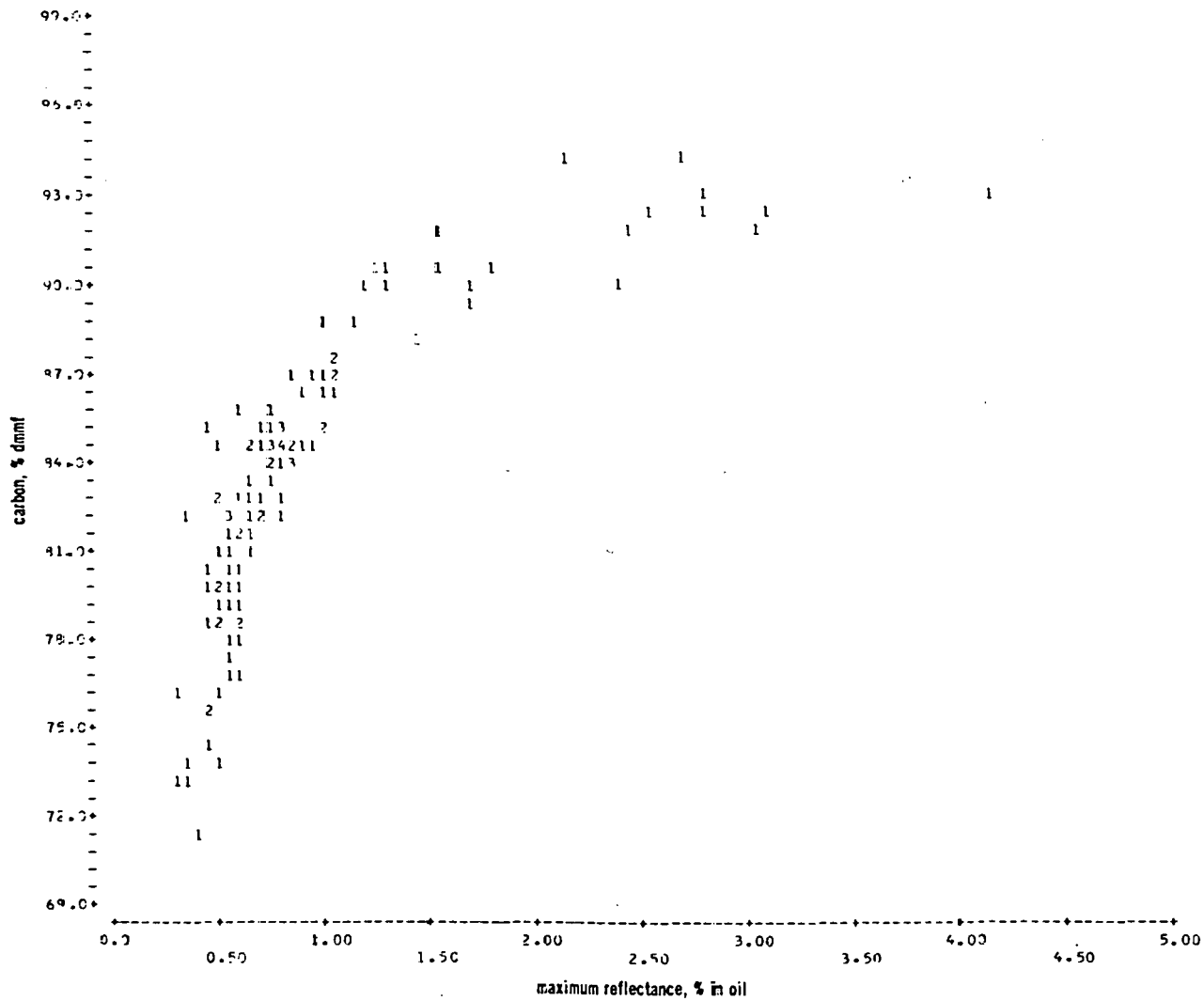


Figure 5. PLOT OF REFLECTANCE VERSUS CARBON FOR U.S. COALS, INCLUDING ANTHRACITES

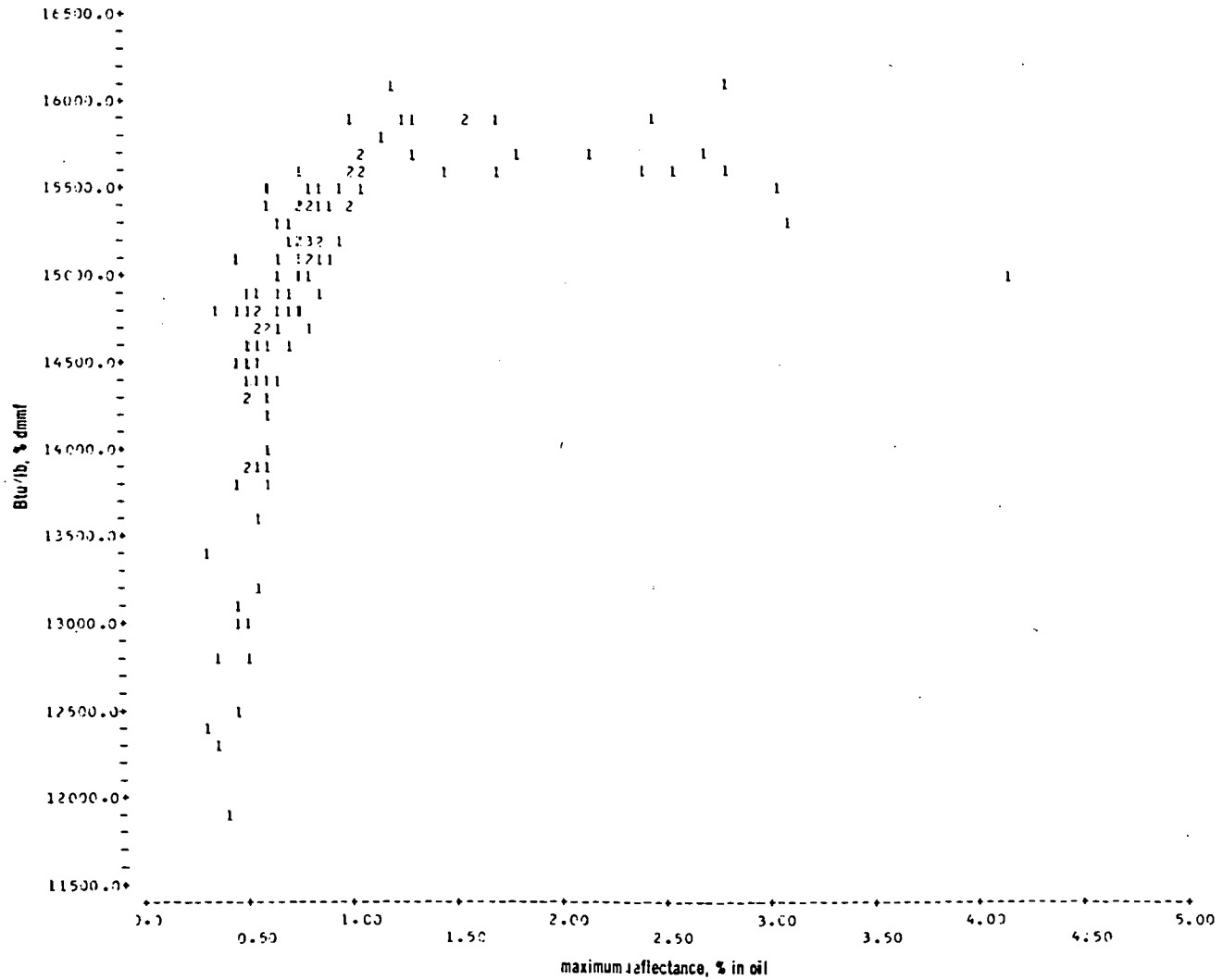


Figure 6. PLOT OF REFLECTANCE VERSUS CALORIFIC VALUE FOR U.S. COALS, INCLUDING ANTHRACITES

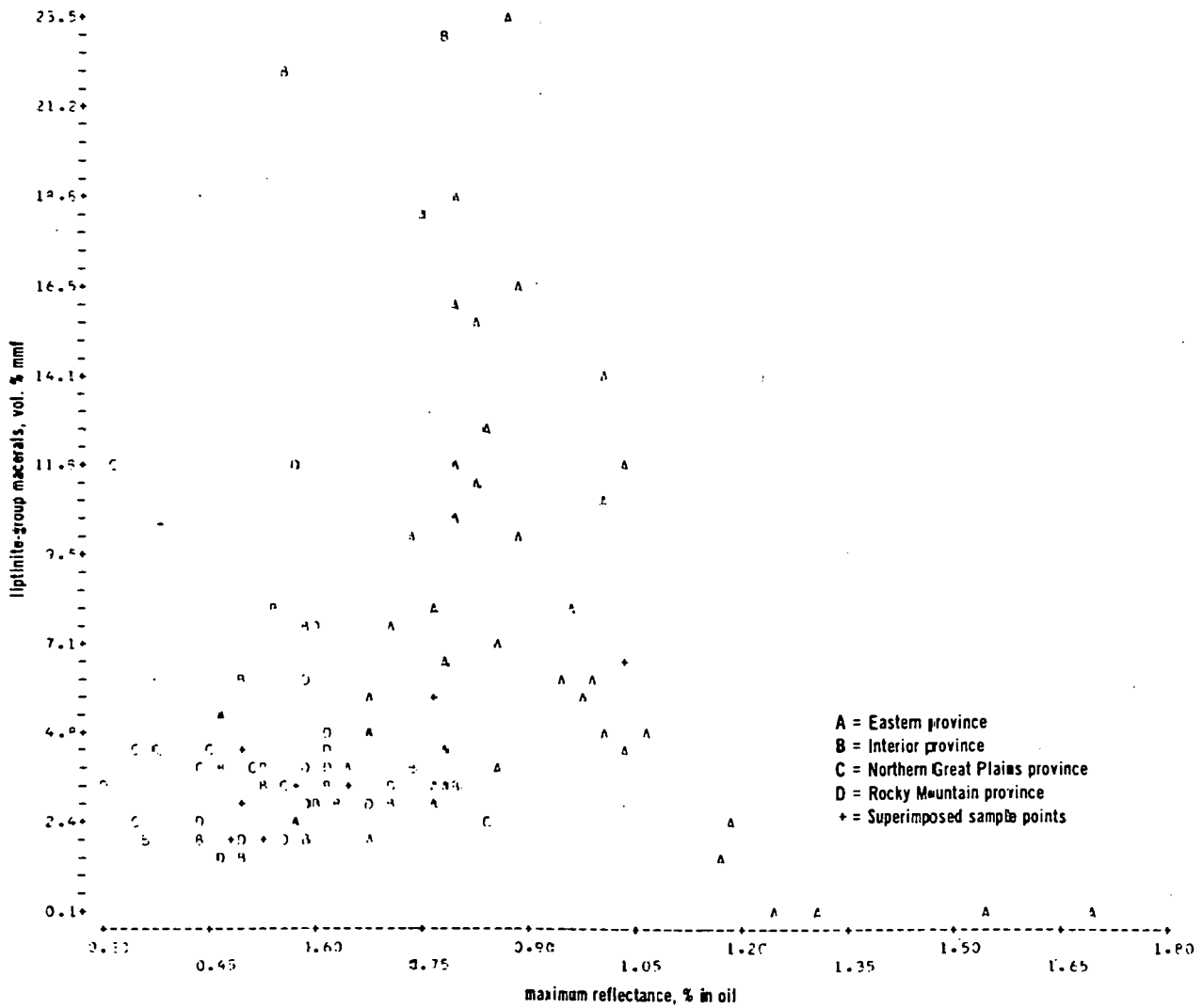


Figure 7. PLOT OF REFLECTANCE VERSUS THE LIPTINITE-GROUP MACERAL CONTENT FOR U.S. COALS

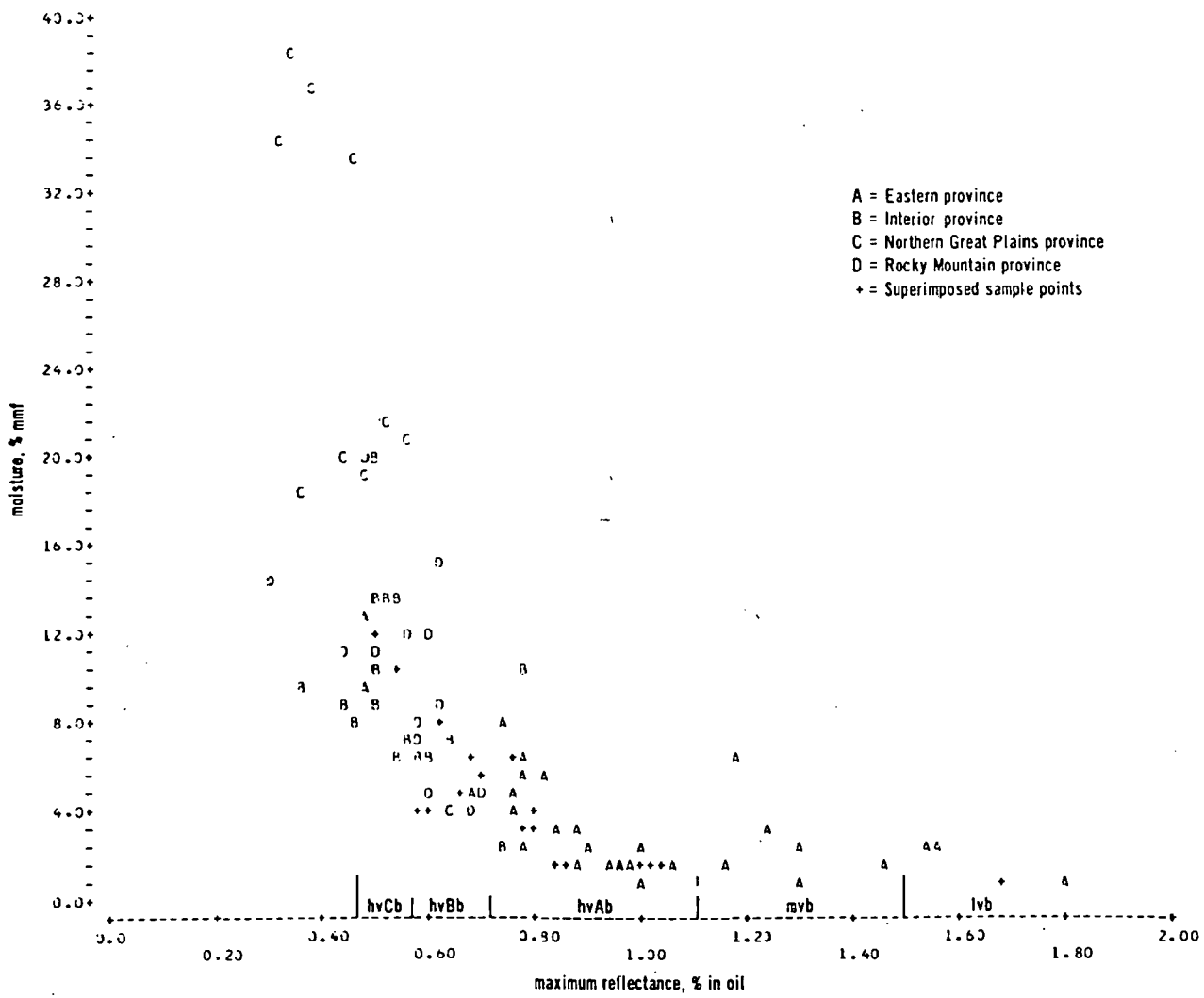


Figure 8. PLOT OF REFLECTANCE VERSUS MOISTURE FOR U.S. COALS

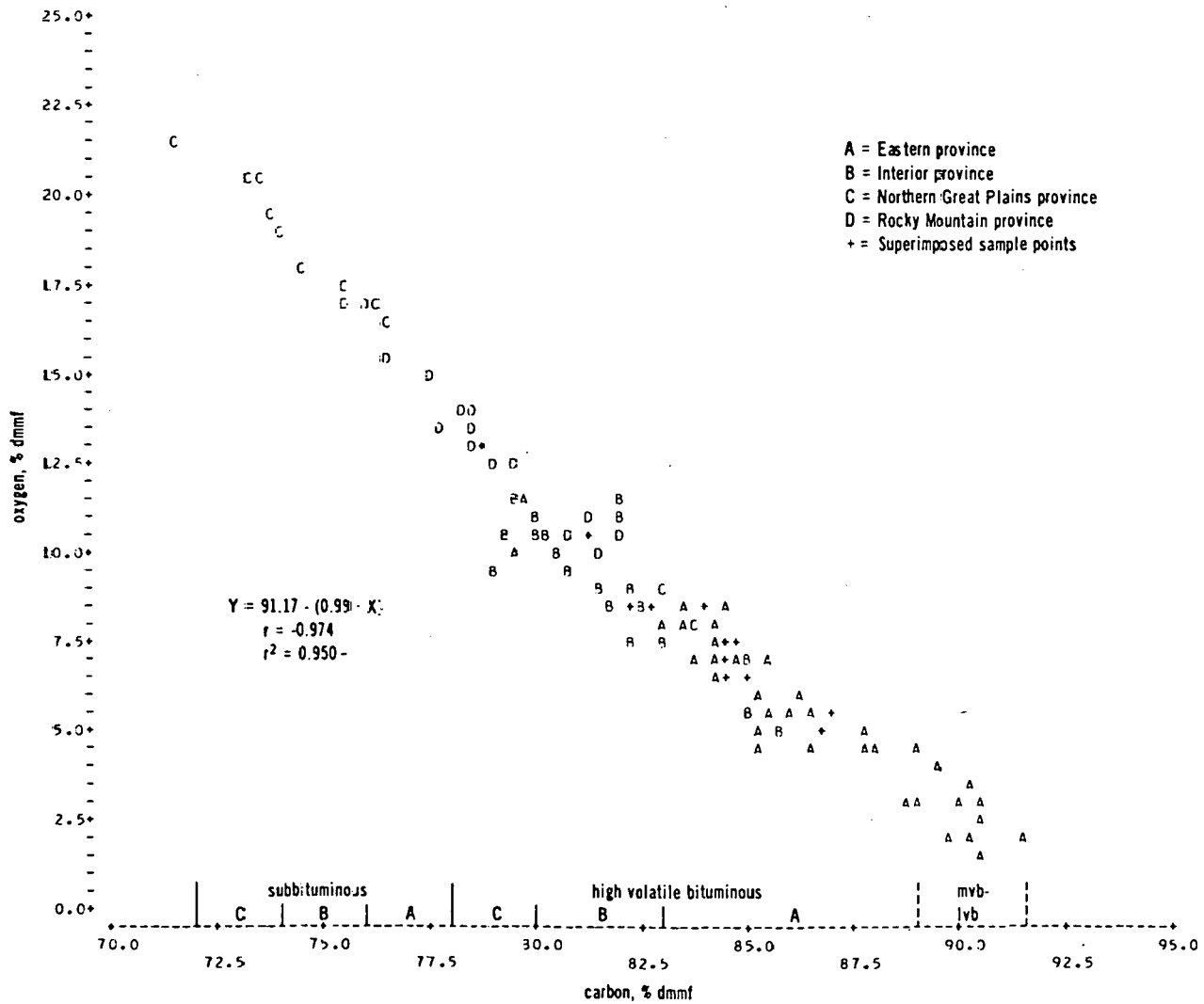


Figure 9. PLOT OF CARBON VERSUS OXYGEN FOR U.S. COALS

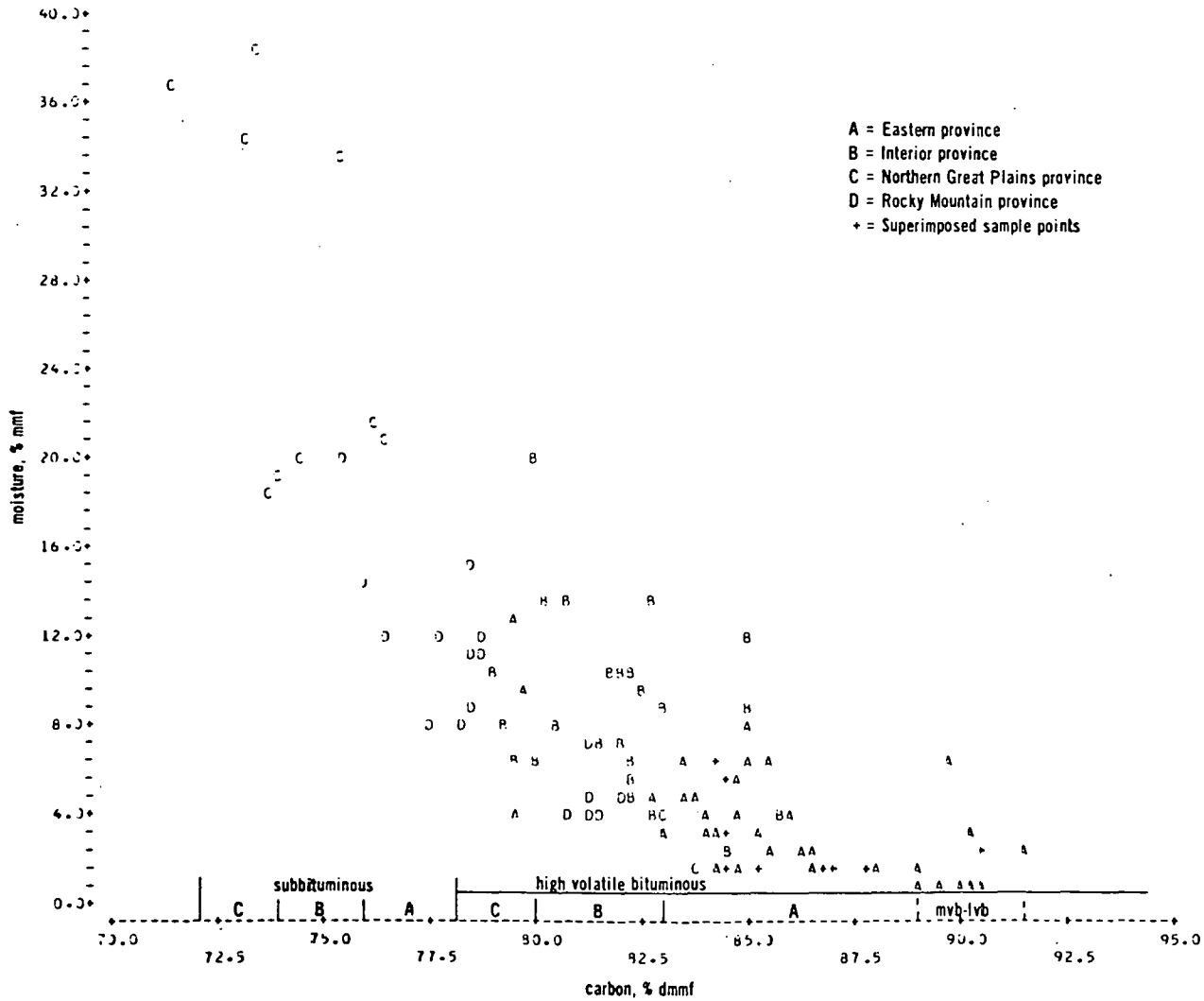


Figure 10. PLOT OF CARBON VERSUS MOISTURE FOR U.S. COALS

## FACET II: COAL BENEFICIATION AND PRE-USE PROCESSING

Coal preparation research is continuing, and a substantial progress report will be forthcoming.

FACET IV-A: REACTOR DEVELOPMENT AND OPERATION

## CHARACTERISTICS OF CHARS PRODUCED BY PYROLYSIS AND COMBUSTION FOLLOWING RAPID HEATING OF PULVERIZED COAL (TASK 23)

### Introduction

Under Task 23, work has been conducted this quarter using nitrogen gas as a pyrolysis medium at 808°C and three size grades of a North Dakota lignite (PSOC-246) as starting materials. This work was intended to verify the previous data on the effects of heat-up and recycling on pyrolysis. The experimental conditions used here are as specified in the last report (March-June, 1977) to ERDA.

### Experimental

If you take one gram of coal and determine the ash content of it by the ASTM method, you find that

$$W_a = A_o W_{coal}/100 \qquad (1)$$

where $W_a$ is the weight of Ash, $A_o$ is the percent ash in the coal, and $W_{coal}$ is the initial weight of coal.

Now if you take 1 g of the coal and subject it to pyrolysis or combustion in the laminar flow reactor, and then subsequently determine the ash content in the residual char by the ASTM method, you find that

$$W'_a = A' W_{char}/100 \qquad (2)$$

where $W'_a$ is the weight of ash, A' is the percent ash in the char, and $W_{char}$ is the initial weight of char.

The basic assumption of the ash tracer method is that ash does not undergo a significant change during pyrolysis or combustion. It, therefore, follows that $W_a = W'_a$ which leads from Equations (1) and (2) to

$$W_{coal} = (A')(W_{char})/A_o \qquad (3)$$

The char yield (Y) at a given time during pyrolysis or combustion can be expressed as a percentage of the original dry, ash-free coal as follows

$$Y = 100[W_{char}(100-A')]/[W_{coal}(100-A_o)] \qquad (4)$$

Combining Equations (3) and (4) yields

$$Y = 100\{[W_{char}(100-A')]/[(A')(W_{char})(100-A_o)/A_o]\}$$

$$= [(100\ a_o)/(100-A_o)][(100-A')/A'] \qquad (5)$$

Hence, weight loss or burn-off, expressed as a percentage of the original dry, ash-free coal is

$$\Delta W \text{ (or } \eta) - 100 - Y \qquad (6)$$

where $\Delta W$ is the weight loss and $\eta$ is the burn-off.

(i) Proximate Ash. Consider the three following cases:

(1) 1 g coal $\xrightarrow{\text{ASTM Ash}}$ 0.1 g ash; $A_u$ = 10.0%

(2) 1 g coal $\xrightarrow[\text{at 800°C, heating rate = 8000°C/sec}]{\text{Pyrolysis or Combustion}}$ 0.9 g char + 0.1 g $V_M$

0.9 g char $\xrightarrow{\text{ASTM Ash}}$ 0.1 g ash; A' = 11.1%

(3) 1 g coal $\xrightarrow[\text{at 808°C, heating rate = 8000°C/sec}]{\text{Pyrolysis or Combustion}}$ 0.88 g char + 0.1 g $V_M$ + 0.02g*

*materials loss due to mineral matter decomposition[1] (for example, $H_2O$ from clays, $CO_2$ from carbonates, sulfur from pyrites, and $SO_3$ from sulfate) or any other reason.

0.88 g char $\xrightarrow{\text{ASTM Ash}}$ 0.08 g ash; A' = 9.1%

(ii) Weight Loss or Burn-Off. Now if the ash contents in the three preceding cases are used as tracers to determine weight loss or burn-off by Equation (6), it is found that:

case (2): $\Delta W$ (or $\eta$) = $\{100-[(100x10)/(100x10)][(100-11.1)/11.1]\}$
= 11.0%

case (3); W (or $\eta$) = $\{100-[(100x10)/(100-10)][(100-9.1)/9.1]\}$
= -11.0%

Cases (2) and (3) can be expressed in general mathematical forms as follows:

First let y = weight of ash in char, x = weight of char, and z = weight of materials lost from mineral decomposition or any other reason as specified in case (3) above.

Now from case (2) we find that ash percent is

$$A' \ (z = o) = 100 \ (y/x) \tag{7}$$

and from case (3) we find that ash percent is

$$(A' \ (z \neq o) = 100 \ [(y - z)/(x - z)] \tag{8}$$

As long as $z > o$ and $x > y$, $A' \ (z \neq o) < A' \ (z = o)$. In the foregoing analysis, $A' \ (z = o) = A_o$ and $A' \ (z \neq o) = A'$.

This analysis shows that: (1) if in the course of pyrolysis or combustion there is a measurable loss of materials due to thermal decomposition of minerals matter or any other reason, the ash percent in the resulting char will be smaller than that in the original coal, unless this effect is offset by a greater extent of pyrolysis or combustion; and (2) if ash percent in the resulting char is smaller than that in the original coal, weight loss or burn-off determined by Equation (6) will be negative.

Weight loss or burn-off in the early stage of pyrolysis or combustion was negative when the 270 x 400 mesh size grade of PSOC-246 was used (Figure 11).[2] These results had never been found in the previous experiments involving pyrolysis of 200 x 270 mesh and larger size grades of PSOC-246 in nitrogen at 808°C.[3] It was shown later[4] that extending the probing process to a much earlier stage of pyrolysis indeed yields negative values of weight loss even when a 200 x 270 mesh size grade is used (Figure 12). Figures 11 and 12 show that negative weight loss or burn-off is offset by a greater extent of combustion and/or pyrolysis. Nevertheless, it is significant that these results show a considerably greater weight loss for the 200 x 270 mesh size grade than for the 270 x 400 mesh size grade. This is contrary to kinetic expectations. It also does not conform to the trend of the results previously obtained in this laboratory[5] covering a mean weight particle size range of 64 to 180 μm for PSOC-246.

Due to the experimental time constraint, the proximate ash contents of chars are ordinarily not determined on the same day a pyrolysis or combustion experiment is carried out. Instead, chars are placed in screw cap vials which are subsequently stored in a desiccator until time is available for determining ash contents. This, therefore, raises the question whether the oxygen picked up during storage is significantly large enough to form oxygen complexes on the char surfaces. If this were to happen, oxygen complexes would perhaps come off as oxides of carbon (that is, carbon monoxide and carbon dioxide), during the ignition test of ash determination. The extra carbon that otherwise would not have come off in the absence of the oxygen complexes would lead to lower yields of ash percent, and hence to greater negative values of weight loss or burn-off whenever applicable. Obviously, this effect would be more pronounced for the air chars than it would be for the corresponding nitrogen chars. Figures 11 and 12 show a reverse trend, which, therefore, seems to rule out this effect.

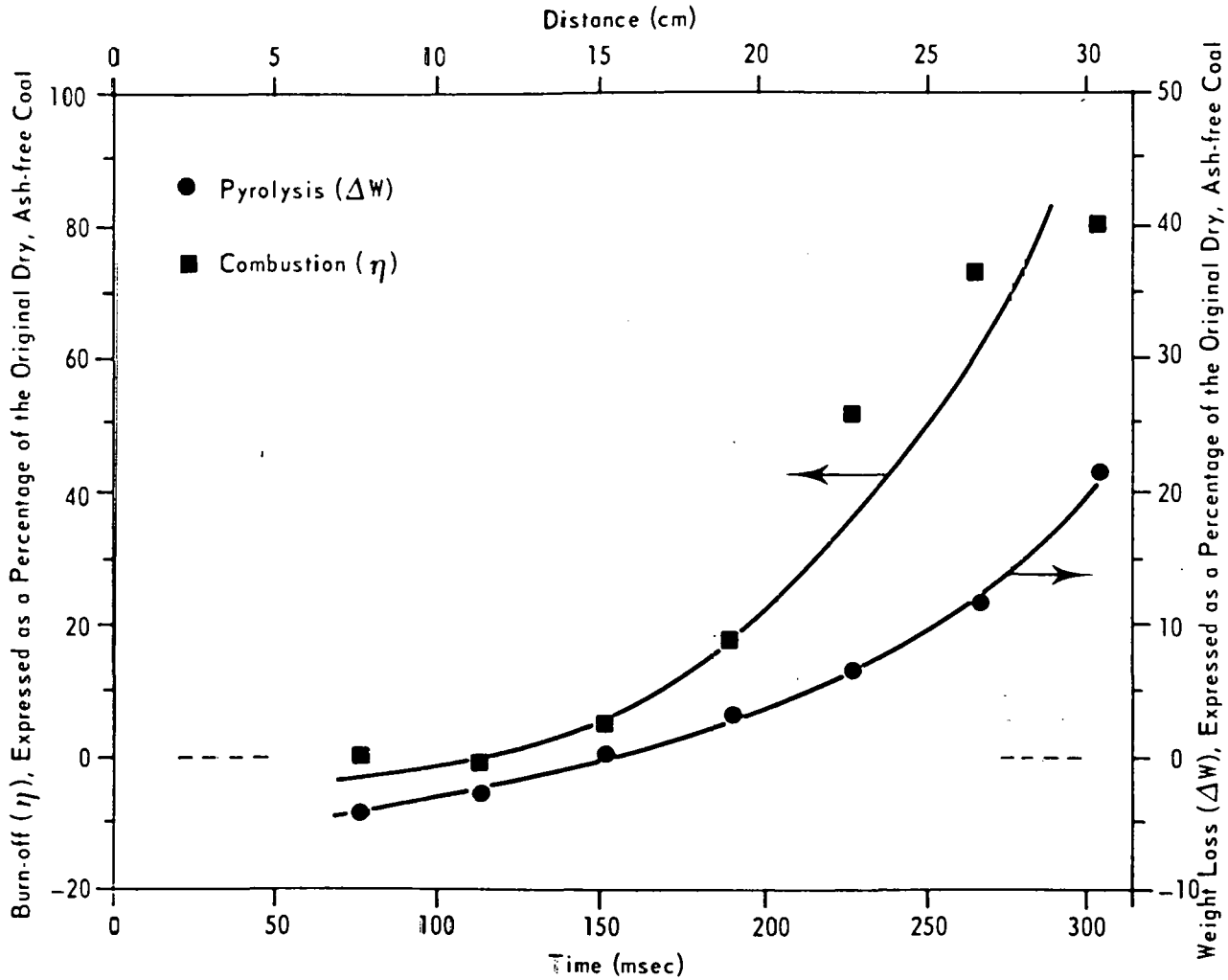


Figure 11. VARIATION OF WEIGHT LOSS ($\Delta W$) OR BURN-OFF ($\eta$) WITH RESIDENCE TIME FOR PSOC-246 COAL (270 x 400) MESH, $\bar{x}$ = 42$\mu$m)

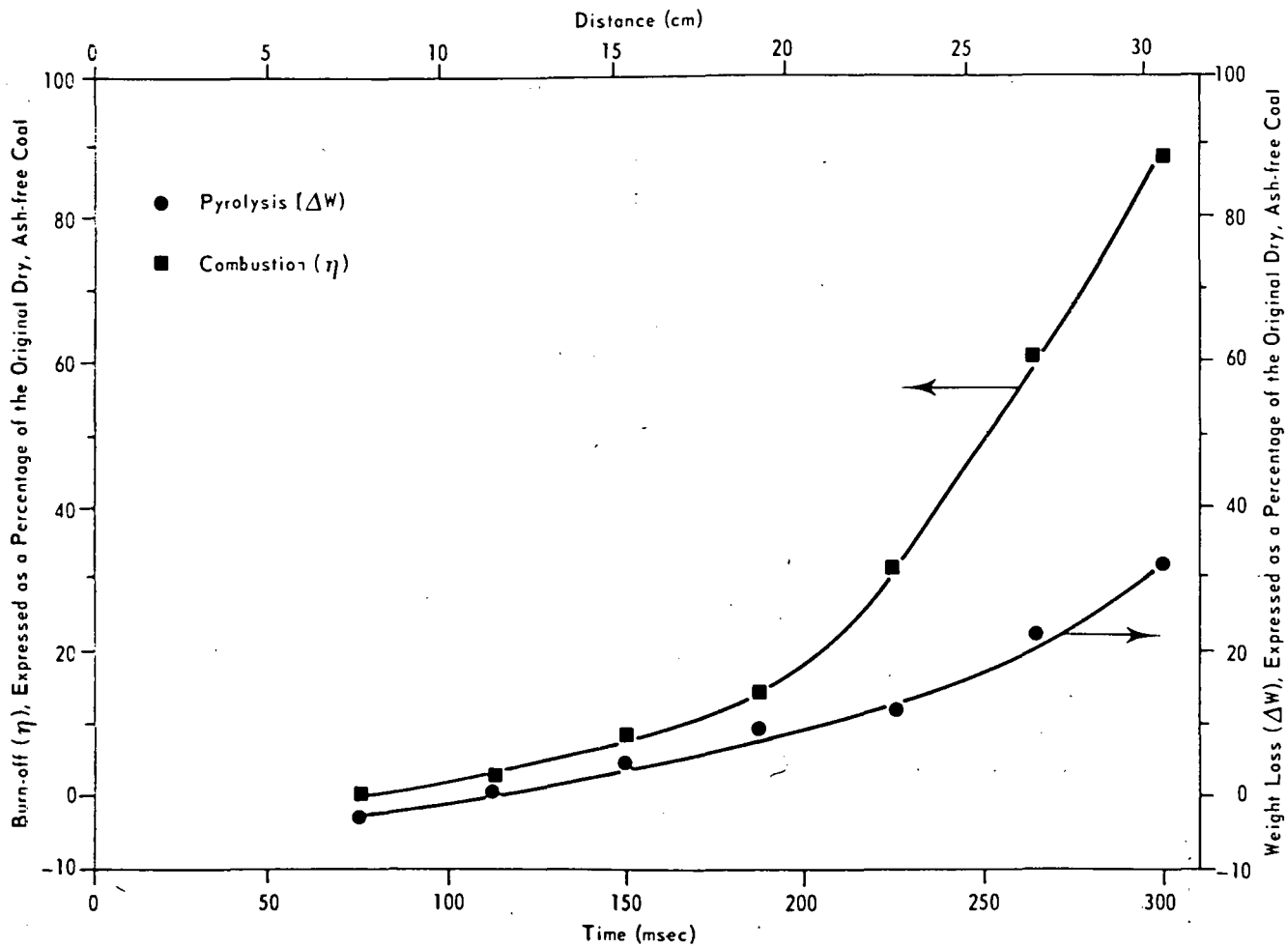


Figure 12. VARIATION OF WEIGHT LOSS ($\Delta W$) OR BURN-OFF ($\eta$) WITH RESIDENCE TIME FOR PSOC-246 COAL (200 x 270 MESH, $\bar{x}$ = 64$\mu$m)

## Effects of Heat-up and Recycling on Pyrolysis

Samples of chars from PSOC-246 were recycled through the furnace one or more times with two objectives in view: to examine the possible influence of heating-up time on weight loss and to determine the feasibility of extending the pyrolysis time by recycling. To test the effects of recycle, the weight loss obtained in a given once-through transit time was compared with the weight loss for the same isothermal and cumulative transit time involving one recycle. Typical results are summarized in Table 4 for four different size grades of PSOC-246. A once-through isothermal transit time of 205 msec could be accommodated involving a preheating period of 95 msec for a total transit time of 300 msec.

Table 4 summarizes the following conditions for comparison. Line 1 gives weight loss of a sample that was removed after 55 msec of isothermal exposure time and then recycled under the same condition. Isothermal exposure time was, therefore, 110 msec, with 190 msec of heating time for a total cumulative residence time of 300 msec. Line 2 gives weight loss for a sample recycled once for the same (190 msec) heating time duration, but the isothermal exposure time was increased to 205 msec for a total residence time of 395 msec. Line 3 is for the once-through sample at 95 msec heating time and 205 msec isothermal time, for a total residence time of 300 msec. The conclusion is self-evident: weight losses were comparable (with some question on the 140 x 200 mesh size fraction) for equal isothermal exposure time (lines 2 and 3); weight losses were clearly far from comparable at equal total residence time (lines 1 and 3). We concluded, as others have previously[6], that there is no detectable or significant weight loss during either the very rapid heating (8000°C/sec) or cooling (27,000°C/sec) periods;[2] even more significant, the pyrolysis mechanism is evidently unaffected at 808°C by the reaction being interrupted. Advantage was taken of these conclusions of the recycling experiments to extend the isothermal pyrolysis time to 1 sec.[2]

Because of the unexpected trend shown in the data depicted in line 1 of Table 4 and the question raised by the results regarding the 140 x 200 mesh size grade of this table (lines 2 and 3), the data given in Table 4 were verified. The average values of weight loss obtained from duplicate runs for this verification are presented in Table 5 for three size grades of PSOC-246. Note that the absolute values of the data in Table 5 are not the same as those in Table 4, even though experimental conditions were the same for both sets of data. This is thought to be due, at least in part, to the fact that the silicon carbide heating elements, placed into the preheater just before the experiments of Table 5 were conducted, may have caused a change in the temperature profile of the gas in the furnace: these heating elements were of different size than the ones previously installed in the preheater by Dr. Bert Philips of Lemont Scientific, Inc. Nevertheless, it is noteworthy that the results of Table 5, in principle, support those of Table 4..

## Effect of Heat-up and Recycling on Weight Loss

All told, it can be re-emphasized that conclusions drawn on the basis of one recycle are, in our opinion, indisputable. However, it is questionable whether the same conclusions would hold for more than one recycle. With this in mind, we plan to carry out the following experiments, using the experimental

Table 4. Effect of Recycling on Weight Loss for PSOC-246 Coal

Old Data

| Recycling Condition | Isothermal Time (msec) | Total time (msec) | Weight loss, % of original daf coal 200x270 mesh | 140x200 mesh | 100x140 mesh | 70x100 mesh |
|---|---|---|---|---|---|---|
| 1. Once | 110 | 300 | 10.1 | 11.4 | 15.6 | 3.7 |
| 2. Once | 205 | 395 | 30.5 | 19.0 | 18.1 | 12.7 |
| 3. None | 205 | 300 | 31.6 | 25.2 | 18.5 | 13.0 |

Table 5. Effect of Recycling on Weight Loss for PSOC-246 Coal

New Data

| Recycling Condition | Isothermal time (msec) | Total time (msec) | Weight loss, % of original daf coal 140x200 mesh | 100x140 mesh | 70x100 mesh |
|---|---|---|---|---|---|
| 1. Once | 110 | 300 | 25.6 | 15.3 | 6.8 |
| 2. Once | 205 | 335 | 30.7 | 29.2 | 18.0 |
| 3. None | 205 | 300 | 32.0 | 30.6 | 20.9 |

conditions given in the previous report to ERDA and a Darco Texas lignite (PSOC-412) as a starting material. (There is not enough PSOC-246 coal remaining to carry out extensive experiments.) Several size grades of PSOC-412 will be recycled through the furnace more than one time such that their cumulative isothermal times match the once through isothermal time of 205 msec. The following cases will be considered: (1) OR30.5, (2) IR20.1, and (3) 2R16.6. In these cases R stands for recycle, the numeral preceding R stands for the number of recycles, and the number following R stands for the distance (in cm) at which reycling is carried out. These cases are such that the cumulative heating time (in msec) is 95, 190, and 285 for case 1, 2, and 3, respectively. If weight losses in these cases are comparable, then it would be safe to postulate that the pyrolysis mechanism is unaffected at 808°C by the reaction being interrupted one or more times.

Dependence of Weight Loss on Particle Size

The experimental data we have applied to the two component kinetic models we have developed show:[2,3] (1) pyrolysis is sensitive to particle size (down to a size of 53 μm) in the first kinetic region, which is governed by the release of component I, and (2) pyrolysis is essentially insensitive to particle size in the second kinetic region which is governed by the release of component II. The reasons for these behaviors are given elsewhere.[2,3] If the particle

size is reduced sufficiently, it is expected that pyrolysis in the first kinetic region will also be independent of particle size. Thus, it has been decided to carry out a systematic study, using PSOC-412. This entails carrying out pyrolysis experiments covering the particle size range 38-250 μm; specifically, the following sieve cuts (in mesh) will be considered: (1) 230 x 400, (2) 230 x 325, (3) 200 x 270, (4) 140 x 200, (5) 100 x 140, (6) 70 x 100, and (7) 80 x 60. These sieve cuts will give us seven mean weight particle sizes against which weight loss in nitrogen at 808°C will be plotted. We believe that this range would give us sufficient information to determine in a more definitive way the dependence of weight loss and where (if at all) particle size invariance on weight loss does occur.

High Temperature Furnace

The building of a 2-in. ID high temperature furnace is continuing. This furnace will allow us to include temperature as one of the variable parameters in this research program.

## EVALUATION OF THE GASIFICATION POTENTIAL OF COALS

Isothermal Reactor (Task 25)

Installation of the pressurized laminar flow isothermal reactor has started. Several components (feed and catch probes, semi-graphic console panel) are being modified by Autoclave Engineers, Inc. Complete assembly is expected to take two months, during which time operational check-out will be conducted on separate major components. Complete system check-out and the research program on pyrolysis will follow.

The design of a hydrogen-safe building i complete, and appropriate steps are being taken to gain final approval and funding to permit construction. No schedule for construction is yet available.

Mechanism of Gasification in a Combustion Pot

During this quarter the study of the reactivity of a Koppers Company coke was resumed and completed. Two size-graded cokes (0.375 in. and 0.625 in.) were used and the results compared with those obtained previously for the size 0.875 in. The data were obtained and analyzed in the same manner as that established previously.[7] For five flow rates (5, 10, 15, 20, and 30 scfm) the temperature distributions through the packed bed were measured using wall thermocouples. The gas concentrations and temperature profiles were quite similar to those obtained previously.[7]

The kinetic coefficients were obtained from a log-linear plot of the concentration term $[(O_2 + CO_2/2)/(1 - CO/2]$ versus time, and the rate constants $n_1$ and $n_2$ were obtained from the slopes of this curve in the combustion and gasification regions. The rate constants thus obtained were then compared with the previous findings. Arrhenius plots ($n^2$ versus 1/T, Figure 13) of the results for the Koppers coke sizes have common slopes corresponding to an activation energy of 48.7 kcal. This value is close

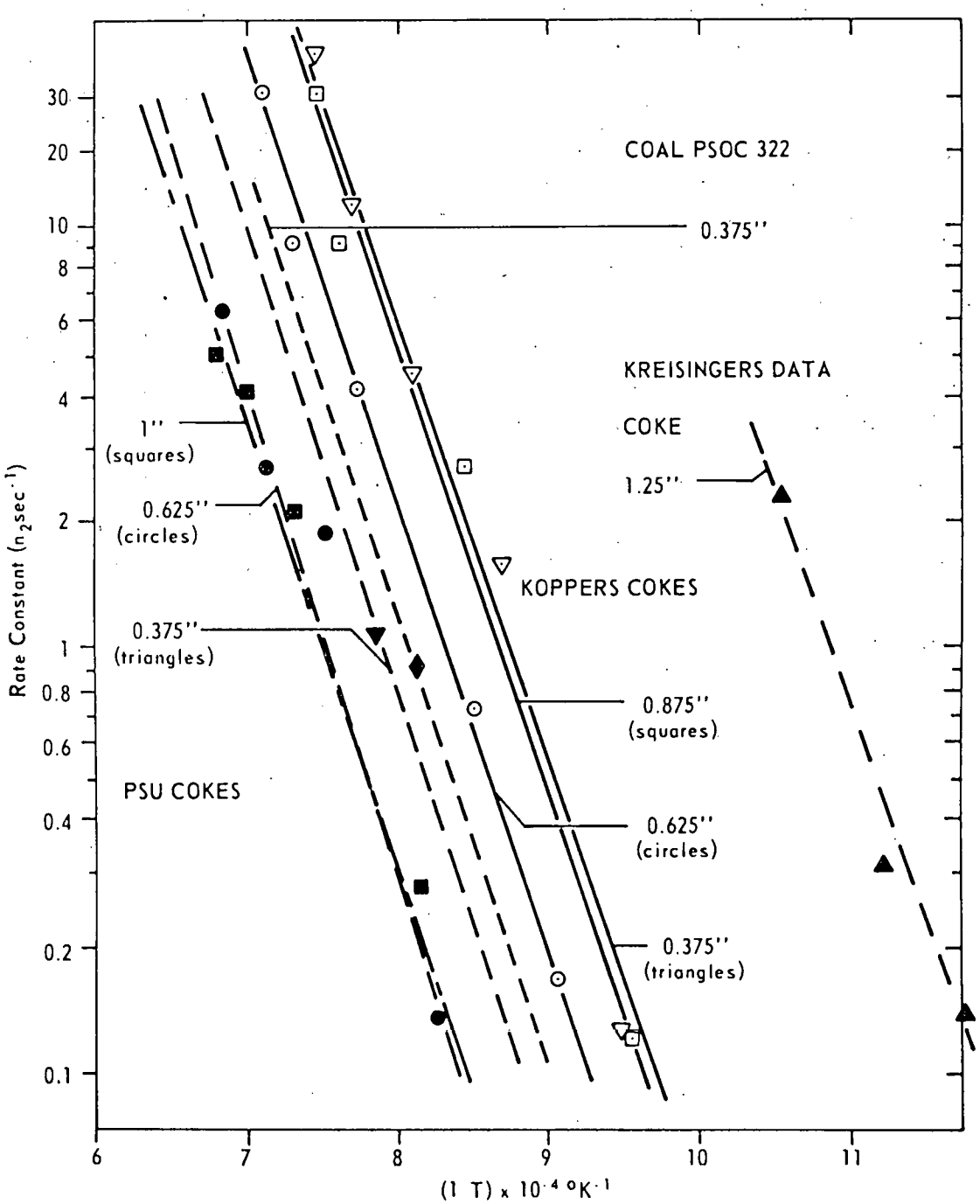


Figure 13. ARRHENIUS GRAPH OF RATE CONSTANT $n_2$ WITH TEMPERATURE FOR KOPPERS COKE E ~48.7 KCAL
Previous data are also included for comparison (Dashed Lines).

to the previously reported 50 kcal[7], further substantiating that the type of coke does not significantly influence the activation energy for the carbon/carbon dioxide reaction in the combustion pot.

Previous analysis showed that the rate constant $n_1$ in the combustion zone is controlled by diffusion and is proportional to $(\text{velocity})^{0.7}$. The rate constants $n_1$ have been plotted against velocity on a log - log scale in Figure 14. The good agreement between theory (illustrated by the dashed line with a 0.7 slope) and experiment is evident. The proportionality coefficients were then determined from the slopes of $n_1$ versus $(\text{velocity})^{0.7}$, Figure 15, where previous analysis[7] has shown that K is related to the particle diameter according to $K = K_0 d^{-0.3 \text{ to } -0.8}$ and $K_0$ is a constant. As indicated in Figure 15, the experimental point corresponding to 30 scfm for 0.375 in. particle was not included in the least squares fit. For such small particles and such velocities the reaction control mechanism is dominated by the kinetic mechanism.

The activation energy of the carbon/carbon dioxide in a non-diffusional system, and the reaction rate constant $n_1$ for the combustion region agree well with the values obtained previously for a different coke. It is apparent that these parameters are essentially independent of coke type.

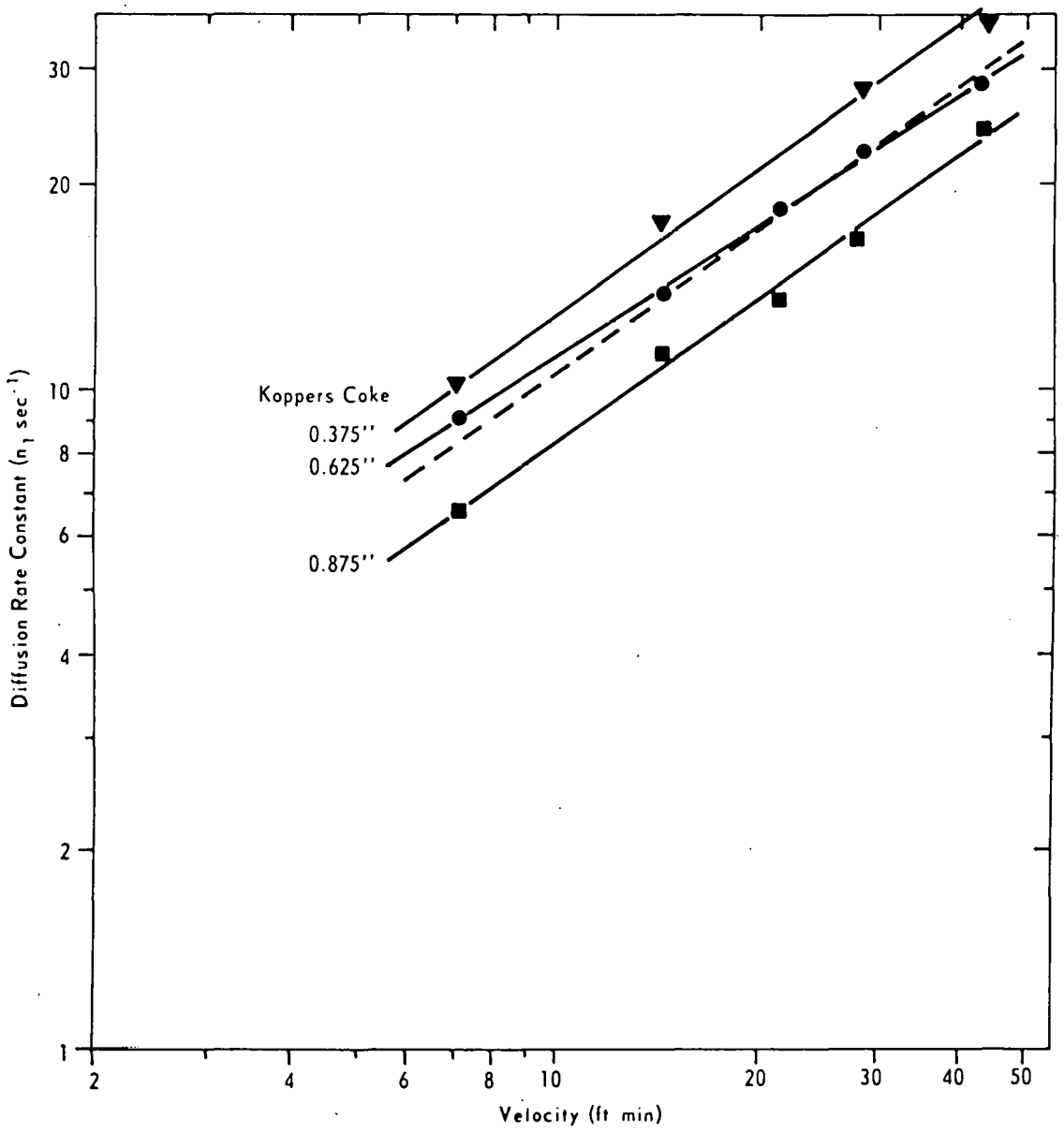


Figure 14. VARIATION OF DIFFUSION RATE CONSTANT $n_1$ WITH VELOCITY FOR THREE DIFFERENT SIZES OF KOPPERS COKE
Dashed line is 0.7 slope.

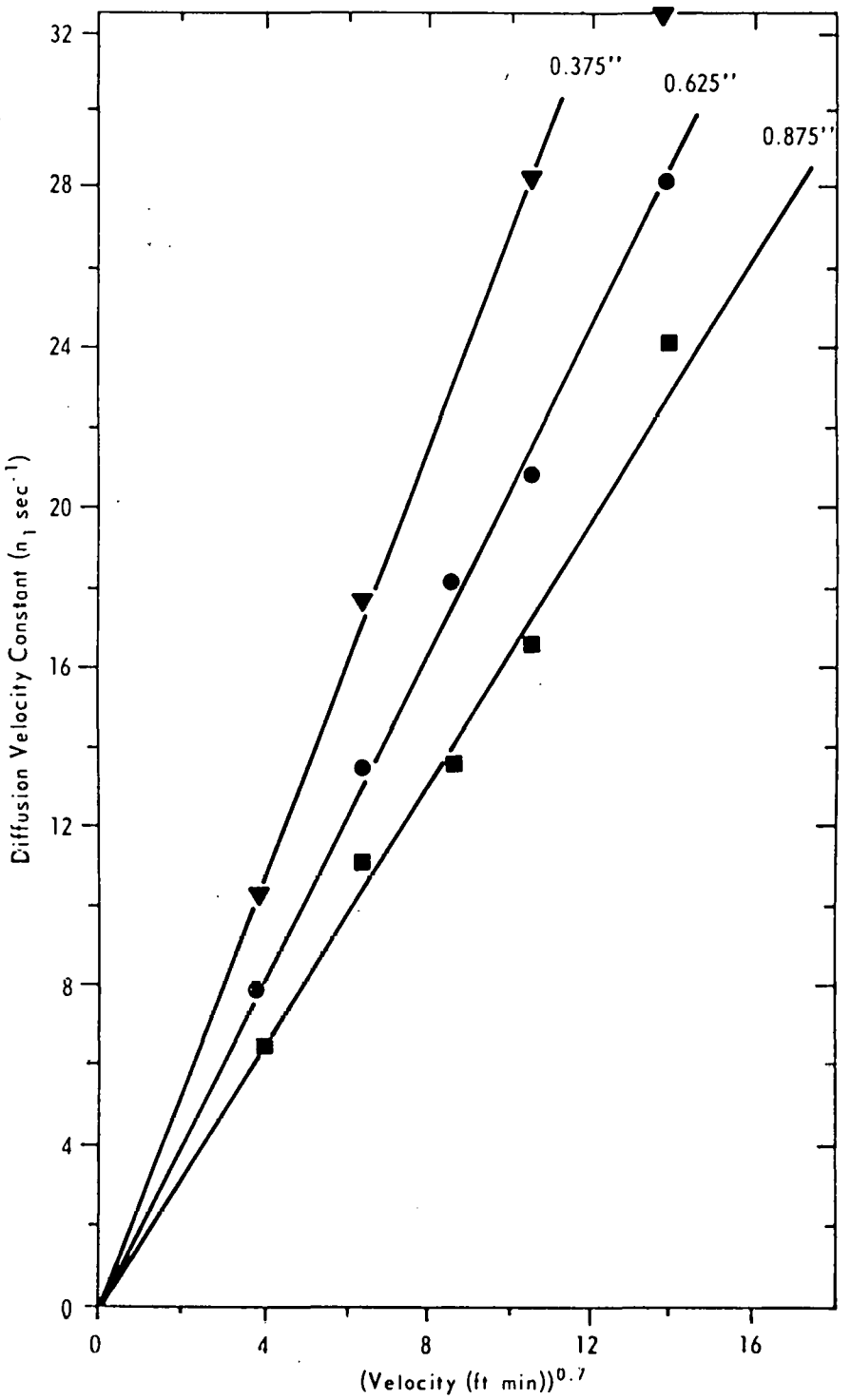


Figure 15. VARIATION OF DIFFUSIONAL RATE CONSTANT $n_1$ WITH (VELOCITY)$^{0.7}$ FOR THREE SIZES OF KOPPERS COKE

## PREOXIDATION OF CAKING COALS TO RETARD THEIR SOFTENING AND SWELLING (TASK 27

### Introduction

Under Task 27, a study is being made into the effects of preoxidation on the agglomerating properties of caking coals. This study is related to the central objective of increasing the reactivity of chars produced from coals which normally cake. By the use of thermogravimetric analysis it has been found that oxygen chemisorption can be followed both quantitatively and reproducibly. In addition it has been shown that oxygen chemisorption is controlled by diffusion through micropores. A significant amount of gasification of a 200 x 250 mesh coal sample has been observed at 200°C in air.

### Experimental

The coals selected for this study are: 1) PSOC-337, a high volatile A coal from the Lower Kittanning seam, Pennsylvania, and 2) PSOC-301, a high volatile A coal from the Splashdam seam, Virginia. Samples of PSOC-337 have been ground and sieved under dry nitrogen (35 x 60 mesh, 100 x 150 mesh, and 200 x 250 mesh). Free swelling index (FSI) determinations have been made on each particle size fraction. The measurements were carried out in a BCR, electrically heated test unit. Apart from the variation in particle size the procedure followed was that described by ASTM (D720 67). The results of triplicate FSI determinations are listed in Table 6. There is an apparent variation in FSI with size range. This is to be expected, to some extent, because of the different packing densities of each size fraction.

One of the major aims of this study is to examine the effect of varying degrees of preoxidation on the swelling properties of caking coals. This requires that a method be used which will allow us to follow the rate of chemisorption of oxygen (from air) onto the coal under controlled heating conditions. A Fisher Thermogravimetric Analyzer (TGA) has been selected for this purpose. By use of the apparatus one can carefully control heating conditions and the sample environment while continuously monitoring weight changes. If chemisorption takes place there will be an increase in weight with time and if gasification occurs then a decrease will be recorded. In these experiments small samples of coal (about 5 mg) are heated to 200°C in dry nitrogen to remove moisture. After constant weight has been achieved air is admitted. At the low temperatures involved (100-200°C) it is extremely unlikely that there will be any diffusional limitations through the sample bed.

The TGA experiments completed to date show much promise. Figure 16 is a plot of oxygen uptake versus particle size of PSOC-337 at 200°C. The results reported have good reproducibility, as can be observed from the plots of duplicate runs with the smallest size fractions (200 x 250 mesh and 100 x 150 mesh). These plots show that the initial uptake of oxygen is most rapid

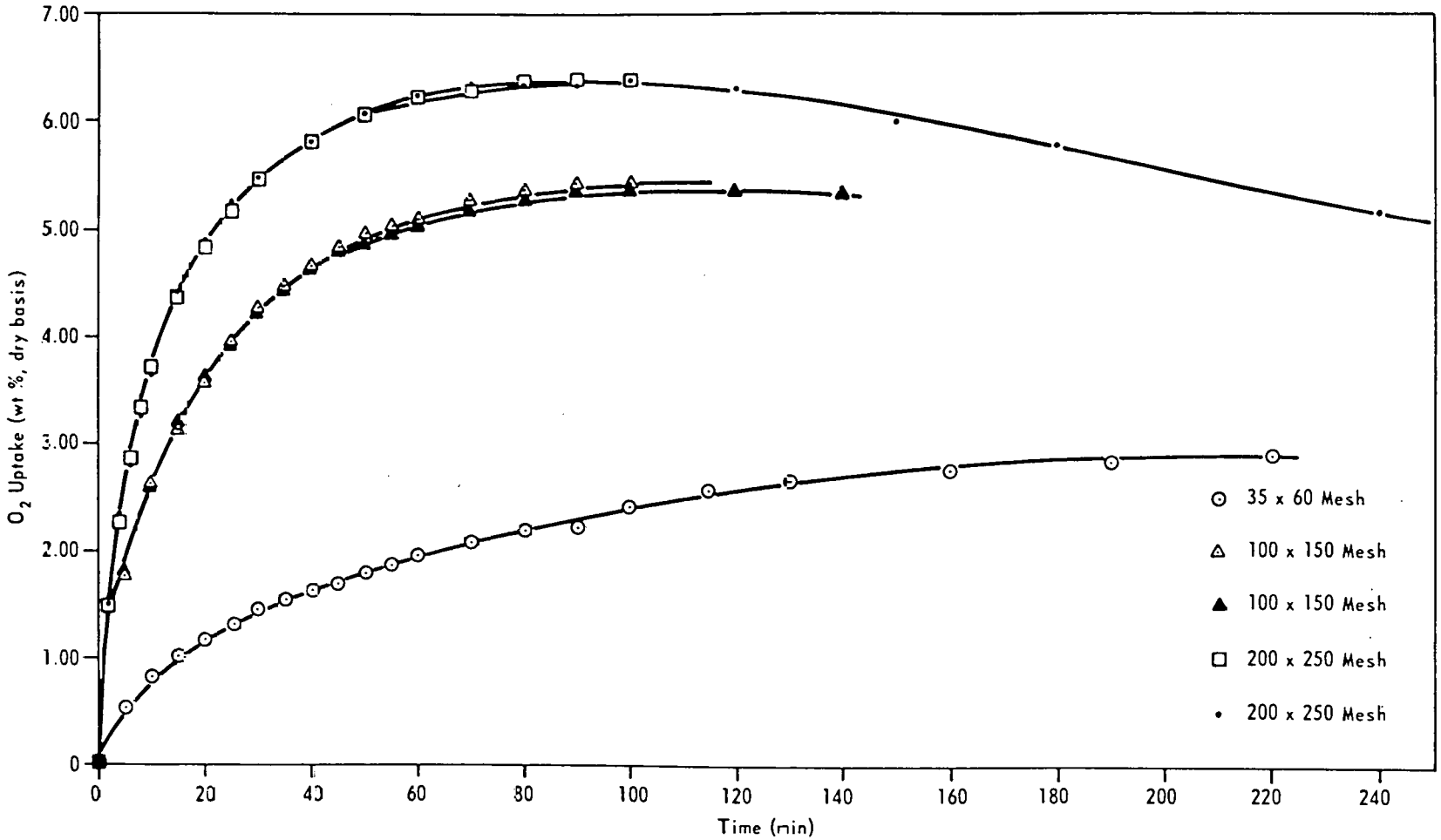


Figure 16. RATE OF OXYGEN UPTAKE AT 200°C AS A FUNCTION OF PARTICLE SIZE FOR PSOC-337

Table 6. Variation of FSI with Particle Size for PSOC-337

| Whole Coal | FSI = 80 |
|---|---|
| Size Fraction | FSI |
| 35 x 60 | 6.5, 6.5, 6.5 |
| 100 x 150 | 8.0, 8.0, 8.0 |
| 200 x 250 | 7.5, 7.5, 7.5 |

for the 200 x 250 mesh size fraction. This observation suggests that the process of oxygen chemisorption is controlled by diffusion through the particles. The amount of oxygen uptake passes through a maximum (at about 90 min) for the 200 x 250 mesh size fraction, indicating that gasification even takes place at low temperatures (200°C). For Figure 17 this plot is continued to 1100 min and that after about 1000 min the net uptake of oxygen is zero. Hopefully, relative rates of chemisorption and gasification for this sample can be estimated by further analysis of this curve.

Returning to Figure 16, the amount of oxygen chemisorbed by the 35 x 60 mesh fraction at 200°C is still increasing after 220 min. The data for the intermediate size fraction (100 x 150 mesh) show that the weight increase due to oxygen uptake appears to reach a constant value after about 90 min. Possibly, either the chemisorption of oxygen has reached a saturation value, or the rates of chemisorption and gasification are equal. In light of the results obtained for the 200 x 250 mesh fraction, this 100 x 150 mesh fraction will be subjected to air at 200°C for a longer period of time to see if, in fact, this plot passes through a maximum.

A series of experiments has been conducted in which the 200 x 250 mesh size fraction has been exposed to flowing air at different temperatures. In these experiments the coal was treated to 200°C in nitrogen and then cooled to the desired temperature (100, 125, 150°C) prior to the admittance of air. Figure 17 plots are made of the weight changes which take place in air at 200, 150, 125, and 100°C for the 200 x 250 mesh sample as a function of time. The initial uptake rate of oxygen increases with increasing temperature. However, as was described previously, at 200°C the weight increase passes through a maximum, after which there is a decrease in weight as gasification proceeds at the expense of chemisorption. At lower temperatures, in the same time scale, no maxima are observed. The data for 150°C show that the amount of oxygen chemisorbed exceeds that at 200°C. From these experiments it would appear that no significant gasification is taking place at these reduced (105°C and less) temperatures.

Further use of the TGA will include the examination of other variables, such as; the effect of grinding in air, the behavior of the larger particle sizes (35 x 60 mesh, and 100 x 150 mesh) at different temperatures, and the effect of moisture on the reactions. TGA runs will be an invaluable facet of this program because they will provide an understanding of the rates of oxygen uptake on these coals, an imperative precursor to the projected coal preoxidation preparations in a fluidized bed.

Work for the next quarter will mainly involve a continuation of the TGA experiments. Projected experiments will examine: 1) the effects of grinding in air on oxygen uptake, 2) the behavior of the 25 x 60 mesh and 100 x

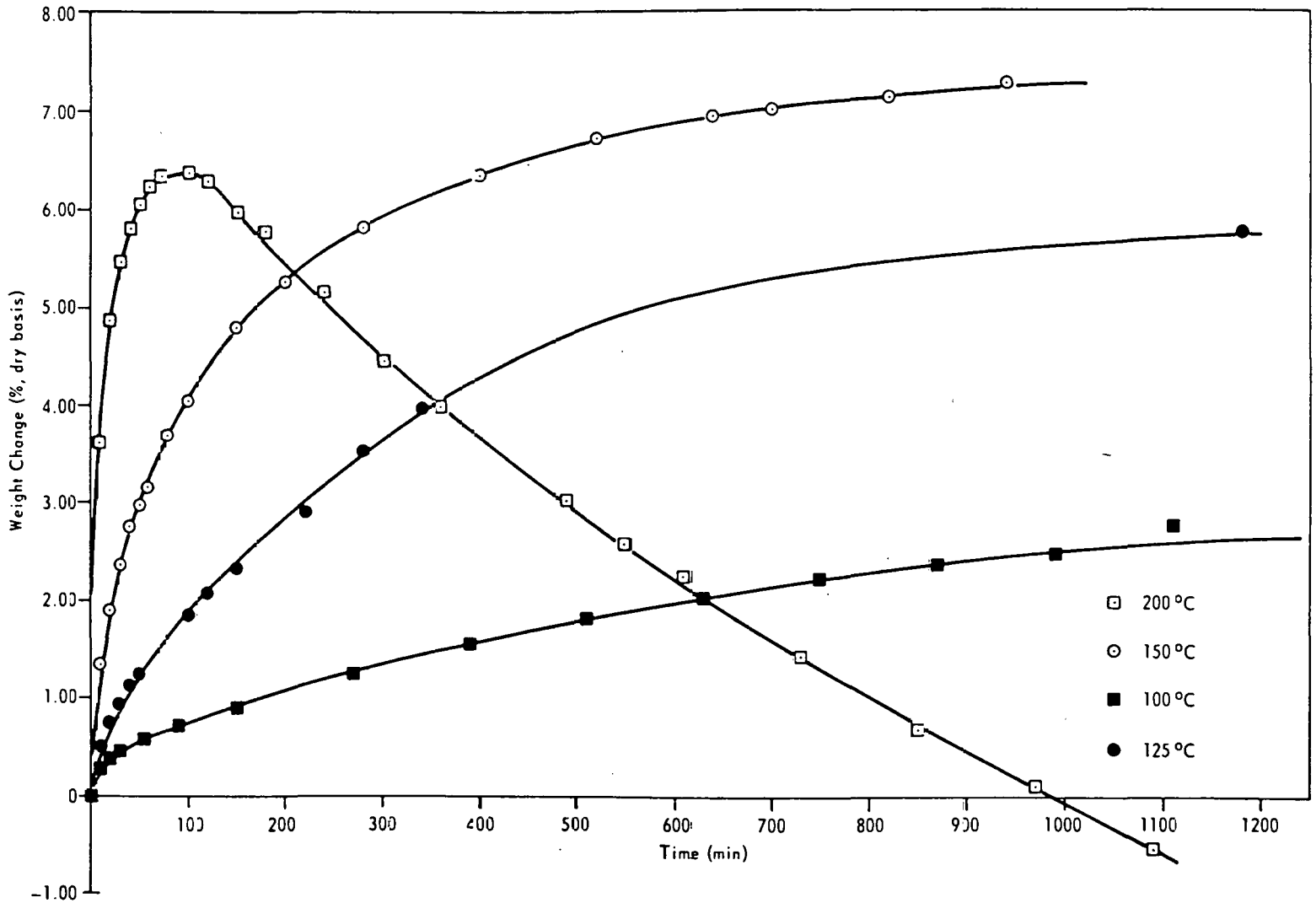


Figure 17. OXYGEN UPTAKE AS A FUNCTION OF TEMPERATURE (200 x 250 MESH PARTICLE, PSOC-337)

150 mesh size fractions at different temperatures, and 3) the effect of water saturation on oxygen uptake. In addition, work has been initiated to optimize fluidization conditions for each of the three particle size ranges. Hopefully, in the near future the TMA apparatus will be operable so that swelling experiments can begin.

## METHANOL AND WATER DENSITIES OF COALS AND CHARS (TASK 27)

### Introduction

Water densities of nineteen coals varying in rank from low volatile bituminous to lignite were determined in the presence of a wetting agent. These densities were lower than those determined in the absence of a wetting agent, but were generally higher than the corresponding helium densities.

### Experimental

Water densities of nineteen coals were determined in the presence of a wetting agent by the procedure followed by Ettinger and Zhupakhina.[8] These workers used a wetting agent composed of a mixture of polyethyleneglycol and monoalkylphenyl ethers. The molecules of the wetting agent, which have hydrophobic hydrocarbon radicals attached to hydrophilic polar surface groups, undergo orientation in water. Ettinger and Zhupakhina suggested that in the case of hydrophobic coals, the polar groups of the wetting agent are turned into the water and the nonpolar groups towards the coal surface. Therefore, subject to penetration by the wetting agent itself, water molecules can penetrate into the coal structure quickly and more completely.

The experimental technique of Ettinger and Zhupakhina[8] involves the following steps. Three-g coal samples (-60 mesh) are transferred into a 100 $cm^3$ measuring flask with the help of a funnel. To remove it, 20 drops of a 1:1 solution of the wetting agent in water are poured directly on the funnel. Care should be taken that no foam formation occurs on addition of the wetting agent. The flask is then half filled with distilled water after which it is placed in a boiling water bath for 30 min and later filled with water up to a graduated mark. The flask is then cooled for 30 min in a thermostated water bath maintained at 20°C after which it is weighed. A blank run, without any sample, is also made by weighing the flask filled at 20°C with water containing the same amount of wetting agent as used with coal. Ettinger and Zhupakhina determined the helium and water densities of fourteen coals having volatile matter contents (daf) in the 1.7 to 44.5 percent range. With three exceptions, the difference between the two methods was less than 1 percent.

In the present study we have used Triton X-100 (iso-octyl) phenoxy polyethoxy ethanol) as the wetting agent. This wetting agent is similar in structure to that used by Ettinger and Zhupakhina.[8] The relevant results are given in Table 7. Water densities in the presence of the wetting agent are invariably lower than those measured in the absence of the wetting agent. Densities in the presence of the wetting agent are lower than the corresponding helium densities for coals varying in rank from anthracite to medium volatile bituminous. For those coals, the difference between the two

Table 7. Helium and Water Densities of Coals

| PSOC Sample No. | ASTM Rank | Carbon (%, daf) (daf) | Density ($g/cm^3$, dmmf) Helium | Water-Wetting Agent | Water |
|---|---|---|---|---|---|
| 177 | Anthracite | 93.5 | 1.541 | 1.534 | 1.566 |
| 85 | Anthracite | 91.3 | 1.391 | 1.389 | 1.400 |
| 318 | LV | 89.5 | 1.326 | 1.326 | 1.526 |
| 236 | MV | 89.5 | 1.288 | 1.279 | 1.302 |
| 135 | MV | 88.4 | 1.336 | 1.322 | 1.350 |
| 254W | MV | 87.2 | 1.301 | 1.288 | 1.465 |
| 268 | HVA | 85.9 | 1.285 | 1.316 | 1.368 |
| 281 | HVB | 83.3 | 1.313 | 1.346 | 1.351 |
| 223 | HVB | 81.3 | 1.297 | 1.363 | 1.397 |
| 238 | HVA | 79.4 | 1.273 | 1.298 | 1.365 |
| 221 | HVA | 79.3 | 1.306 | 1.336 | 1.476 |
| 212 | HVC | 79.0 | 1.295 | 1.360 | 1.327 |
| 288 | HVC | 78.2 | 1.319 | 1.368 | 1.359 |
| 312 | HVC | 77.7 | 1.326 | 1.380 | 1.432 |
| 233 | HVC | 77.4 | 1.315 | 1.359 | 1.462 |
| 230 | Sbb-B | 75.3 | 1.333 | 1.430 | 1.424 |
| 248 | Sbb-A | 75.2 | 1.343 | 1.418 | 1.558 |
| 242 | Sbb-B | 73.9 | 1.340 | 1.429 | 1.649 |
| 246 | Lignite | 70.9 | 1.373 | 1.511 | 1.563 |

density values is less than 1 percent. For coals lower in rank than medium volatile bituminous, the helium densities are lower than the water densities in the presence of the wetting agent; the difference in the two densities, which varies between 2 and 10 percent, shows a random variation with coal rank.

From the results of the present investigation, it may be concluded that only in the case of coals varying in rank from anthracite to medium volatile bituminous, the true densities, that is the density of the solid phase, can be determined by the Ettinger and Zhupakhina[8] technique as well as by the displacement of helium; whereas for the lower rank coals true densities can only be measured by helium displacement.

In this laboratory, particle densities of coals and chars are determined by mercury displacement. Ettinger and Zhupakhina[8] have reported that particle density of coal can also be determined by 'silanization', which involves coating the coal surface with a very thin, transparent film of an organosilicon compound, The thin film is impervious to water and has practically no influence on the weight or volume of the coal particles. Particle densities of nineteen coals of different rank will be measured by the silanization technique; these densities will be compared with the corresponding mercury densities.

## CATALYSIS OF CHAR GASIFICATION (TASK 30)

### Introduction

Preliminary studies have been conducted regarding the effect of bed height and particle size on reactivity in air of Saran char as well as a sample loaded with 1 percent platinum.

### Experimental

Studies show that the gasification rates of carbonaceous solids depend on three main factors: 1) density of carbon sites located at the edges of planar regions or crystallites, 2) chemical form, type, and particle size of catalytic inorganic impurities, and 3) accessibility of the active sites and catalytic material to the reactant gases.

During the course of a gasification reaction the density of edge sites, or active surface area, the total surface area, and pore size distribution of the carbon, as well as the degree of dispersion and possibly the chemical form of the catalytic impurities, change continuously. In order to fully understand the mechanism of char gasification, it is necessary to understand the changes occurring in the above factors as a function of carbon burn-off. A meaningful interpretation of the data from such a study is possible only if reactivity of the char is chemically controlled rather than diffusion controlled. Besides, catalytic effects of impurities invariably associated with coals and coal chars would also greatly complicate interpretation of the data. Because of the problems associated with these impurities, the char support used in this study was prepared by carbonizing (at 900°C) Saran, which is a copolymer of polyvinylidene chloride and polyvinyl chloride in a ratio of about 9:1. Saran char is very pure, highly microporous in nature, and has a structure similar to the coal-derived chars. The metal catalyst chosen for this study was platinum since simple analytical techniques are available for determining its degree of dispersion. It was decided to study the gasification behavior in air.

Before any work on the rather complicated platinum-carbon could be undertaken, an understanding of the development of active and total surface area during the gasification of Saran char itself was necessary. Obviously, in the proposed study gasification kinetics should be controlled essentially by intrinsic chemical reactivity of the char and not by any diffusional effects. Therefore, the first step was to ascertain the experimental conditions under which reactivity was independent of particle size.

The effect of reaction temperature on gasification of 70 x 100 mesh Saran carbon in air is shown graphically in Figure 18. In a few exploratory runs, at each reaction temperature studied, gasification behavior was essentially independent of bed height. That is, resistance to diffusion of reactant molecules down through the bed was minimal. The extent of gasification at any reaction time is favored by an increase in reaction temperature (Figure 18), as expected. Since reaction rate at 475°C is neither too fast nor too slow, this temperature was used as the reaction temperature in subsequent reactivity work.

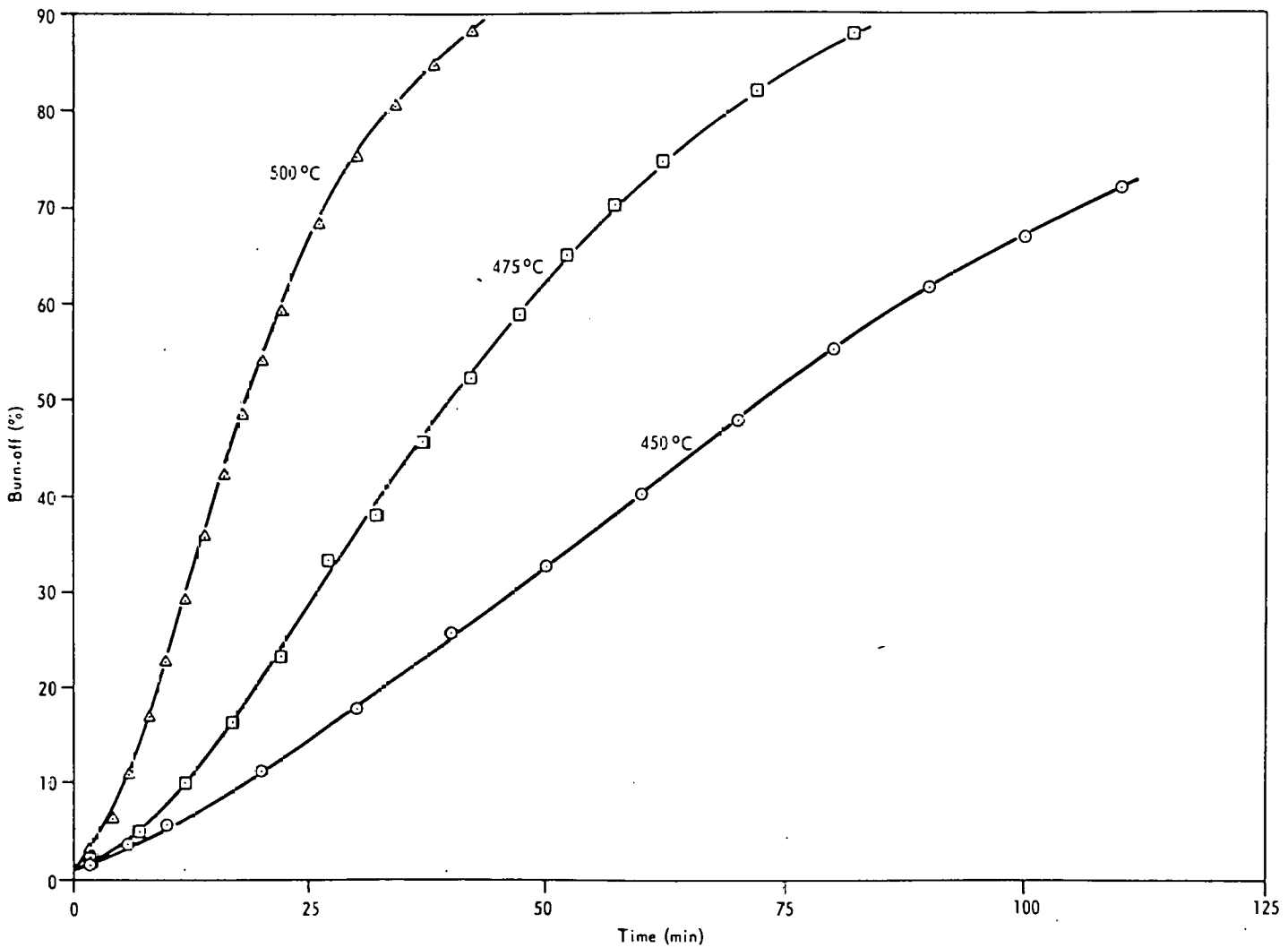


Figure 18. BURN-OFF CURVES OF 70 x 100 MESH SARAN CARBON IN AIR AT DIFFERENT TEMPERATURES

The effect of particle size on reactivity of Saran char was studied next at 475°C. The particle sizes studied were 70 x 100 and 140 x 200 mesh. For both particle size fractions, the data points approximately fitted on the same burn-off versus time curve, which indicates the absence of any significant mass transport control of the gasification process. That is, gasification rates are controlled almost solely by intrinsic chemical reactivity of char.

The effect of 1 percent platinum loading on 70 x 100 mesh Saran carbon on reactivity at 475°C is brought out in Figure 19. Relevant data for Saran char itself are also plotted in Figure 19 for the sake of comparison. Over the entire range of carbon burn-off platinum catalyzes the gasification in air. The effect of particle size of one percent platinum loaded Saran carbon on reactivity at 475°C was studied for 70 x 100 and 140 x 200 mesh fractions. The latter size fraction was prepared by grinding (in a ceramic mortar) the 1 percent platinum-loaded 70 x 100 mesh fraction. The larger size fraction, contrary to expectations, was more reactive during gasification than the smaller 140 x 200 mesh fractions. This is presumably due to segregation of platinum particles during grinding.

In order to confirm whether the reactivity of the 70 x 100 mesh fraction of one percent platinum-loaded Saran char was independent of particle size and, hence, intraparticle diffusion, the following alternate approach was used. Upon comparison of burn-off versus time curves for Saran char at 500°C (Figure 18) and 1 percent platinum-loaded sample at 475°C (Figure 19), at any stage the gasification rate is higher for Saran char. Therefore, it is reasonable to assume that if gasification rates of Saran char itself at different burn-off values at 500°C are independent of bed height, the rates should also be independent of particle size for the platinum-loaded sample. The data for two different particle sizes for Saran char plotted in Figure 20 confirm this view.

Because at least 0.5 g sample will be needed to determine active and total surface area, conventional TGA units cannot be used for producing such quantities when gasification rates are independent of bed height. As an alternative, a horizontal tube furnace with a sufficiently long, constant temperature zone will be used so that about 2 g Saran carbon can be spread in a graphite boat in a thin layer to minimize bulk diffusional effects. Reactivity of the sample to air, that is, the extent of gasification as a function of time, at predetermined reaction temperatures will be monitored by analyzing the product gases by chromotography. Using this technique, attempts will be made in the next quarter to produce burn-off versus time curves which are more or less superimposable on those obtained under similar experimental conditions using the TGA technique.

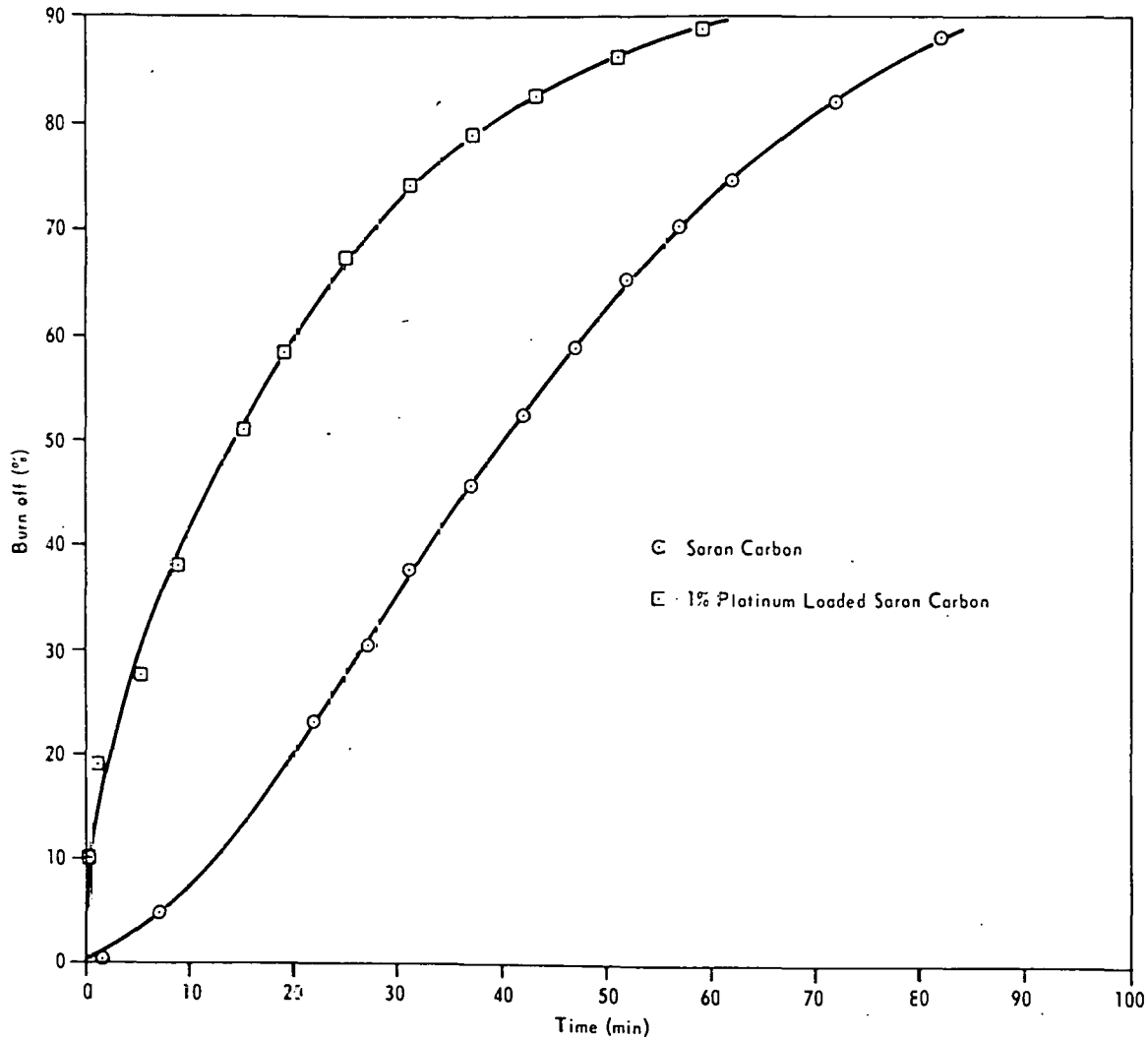


Figure 19. EFFECT OF 1 PERCENT PLATINUM LOADING ON BURN-OFF CURVE OF 70 x 100 MESH SARAN CARBON AT 475 °C

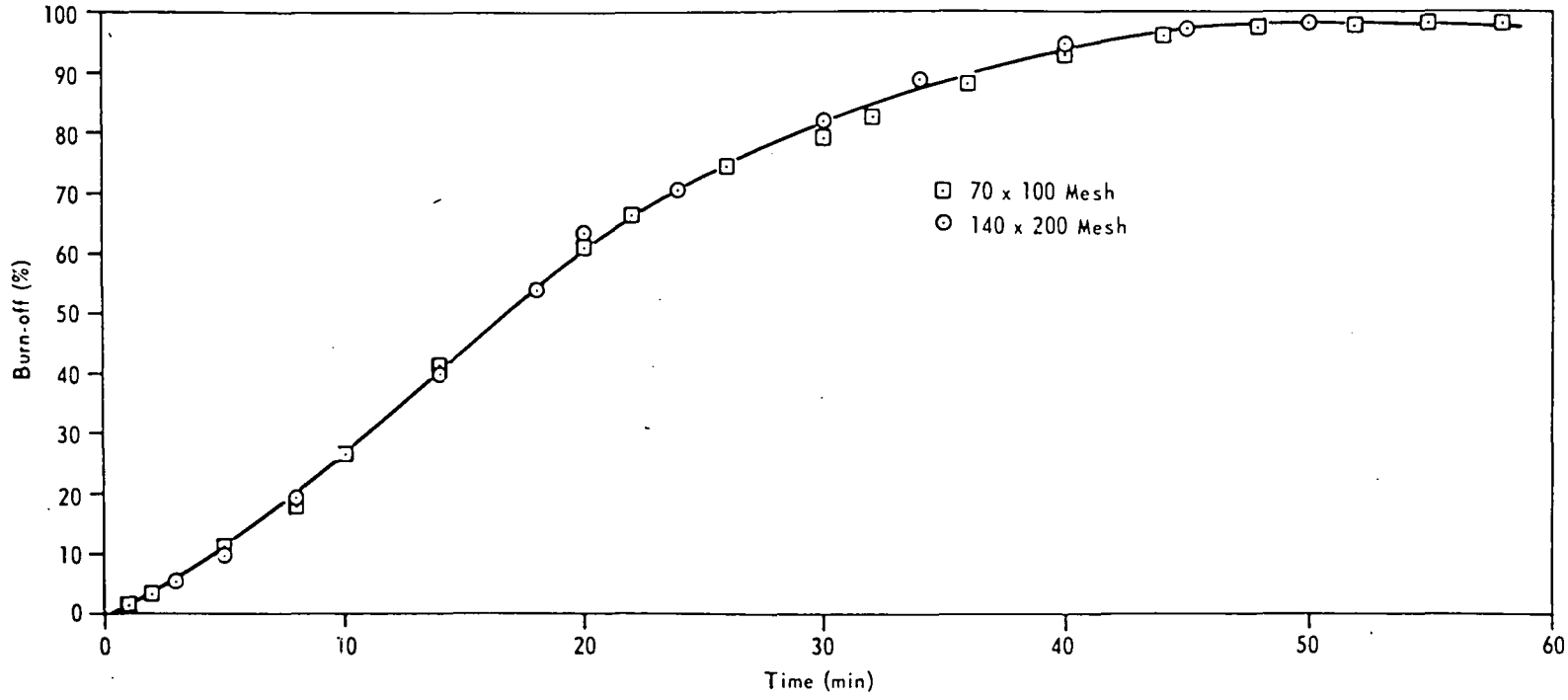


Figure 20. EFFECT OF PARTICLE SIZE ON BURN-OFF CURVE OF SARAN CARBON AT 500 °C

## FACET IV-F: DIFFERENTIAL SCANNING CALORIMETRY

### CHEMISORPTION OF OXYGEN ON CARBONACEOUS SOLIDS (TASK 31)

#### Introduction

Under Task 31, the DSC and TGA techniques have been used to calculate the heat of oxygen chemisorption ($\Delta H$), at 100°C on an air-activated Saran carbon. Dependence of $\Delta H$ (kcal/mole) on surface coverage ($\theta$) as well as on desorption temperature in the range 450-905°C was investigated. For desorption temperatures of 450, 500, 550, and 600°C used to clean the carbon surface (prior to oxygen chemisorption) values of $\Delta H$ are: 57 ± 2, 55 ± 3, 64 ± 1, and 74 ± 3 kcal/mole, respectively. For desorption temperatures of 600°C or above, $\theta$ varies between 0.46 and 0.75; however, $\Delta H$ is almost constant and amounts to 74 ± 3 kcal/mole.

#### Experimental

The dependence of $\Delta H$ (kcal/mole) on surface coverage ($\theta$) was studied at 199°C for the air-activated sample brought to the 63.8 percent level of carbon burn-off. This study was done on several samples treated two different ways:

1. Fresh samples whose surfaces had been once subjected to different given desorption temperatures and finally allowed to react with oxygen at 100°C.

2. Recycled samples, that is, those which had been (a) subjected to certain desorption conditions, (b) reacted with oxygen at 100°C until reaching the saturation condition, and (c) again desorbed via identical conditions similar to (a).

Whether the samples were fresh or recycled, values of Q were measured during the first 28 min reaction time. However, for each TGA run, measurements of w (mg oxygen/g C) were continued until the surface was completely covered with oxygen, and hence no further significant weight increase was detected. These long-term runs were required to determine the total amounts of oxygen uptake on the samples, and, therefore, to calculate the corresponding values of $\theta$. Furthermore, each value of $\Delta H$ (kcal/mole) at a given reaction time was calculated from the corresponding values of Q (cal/g C) and w (mg oxygen/g C).

#### Dependence of $\Delta H$ on $\theta$ for Fresh Samples

For these experiments, a fresh sample was used at the beginning of every experiment. For each DSC or TGA run, the sample was evacuated, flushed with nitrogen at a constant rate of 45 cc/min, heated at 20°C/min up to a given desorption temperature in the range 600-700°C (maximum operating temperature for the DSC cell is 720°C), and finally kept at a particular desorption temperature for 30 min. Thereafter, the sample was cooled to room temperature, held isothermally at 100°C, and then allowed to react with oxygen at 45 cc/min. Values of Q and w were determined experimentally,

while values of $\Delta H$ and $\theta$ were thereafter calculated. The results are given in Table 8 for desorption temperatures of 600 and 700°C. As one can see, values of $\Delta H$ and $\theta$ for both desorption temperatures are very close. Therefore, it was essential to perform an additional experiment where lower values of $\theta$ could be reached. For this purpose, an auxiliary vertical quartz reactor (with an upper inlet and a lower outlet for nitrogen) was used to heat the sample at temperatures above 700°C. The sample was heated in nitrogen at 20°C/min up to 950°C, then kept at this desorption temperature for 30 min, and finally cooled to room temperature. This treatment is believed to clean the carbon surface extra, via desorption of carbon monoxide and carbon dioxide which is more pronounced at 950°C than at 700°C. The calculated values of $\theta$ (see below) for this run confirmed the assumption.

At the end of this treatment, part of the sample was transferred to the DSC cell and the rest was used for a TGA run. Once more, in each apparatus, the sample was heat treated up to 600°C according to the conventional procedure described earlier in this report. Values of $\Delta H$ and $\theta$ at 100°C for oxygen chemisorption were calculated and are presented in the last column in Table 8. It is concluded from this table that for desorption temperatures of 600°C or higher, values of $\Delta H$ (kcal/mole) are almost constant and scattered around a value of 74 ± 3 kcal/mole. This is true for values of $\theta$ ranging between 0.46 and 0.75. It might be mentioned, in this connection, that an experimental error of ± 2 to 3 percent is allowed while measuring the values of either Q or w. This leads to an accumulated error of ± 1 to 9 percent for the calculated values of $\Delta H$.

Further attempts were made to investigate the dependence of $\Delta H$ on $\theta$ for coverages below 0.46 or above 0.75. The former case, that is, for values of $\theta < 0.46$, has been rejected at the present time because of the limitations presented by the DSC cell (maximum operation temperature is 720°C, lowest pressure is 0.1 torr). The latter case, that is values of $\theta > 0.75$ were examined by heating the sample at degassing temperatures below 600°C or by performing successive adsorption-desorption cycles on the same sample for desorption temperatures of 500 to 700°C. The results for temperatures below 600°C are given in Table 9. For each desorption temperature, values of $\Delta H$ are almost constant. Thus, for each desorption temperature, although $\theta$ increases by about 7 to 9 percent, $\Delta H$ is independent of coverage. $\Delta H$ values are significantly lower than those following desorption at temperatures of 600°C and above.

Dependence of $\Delta H$ on $\theta$ for Recycled Samples

Adsorption-desorption cycles were studied for desorption temperatures of 500, 600, and 700°C. For each temperature, a fresh sample was used at the beginning of the first cycle. Each fresh sample underwent the conventional heat pretreatment procedure up to the desired desorption temperature. Thereafter, the sample was kept at this temperature for 30 min, and then cooled down to room temperature. Following this, the sample was allowed to react with oxygen at 100°C until reaching saturation conditions. Values of $\theta$ and $\Delta H$ (kcal/mole) were calculated as described earlier for a fresh sample. After reaching the saturation conditions, the sample was cooled to room temperature in a nitrogen atmosphere, evacuated, flushed with nitrogen, and

Table 8. Dependence of ΔH (kcal/mole) at 100°C on Surface Coverage (θ) (Desorption Temperatures = 600, 700, and 950°C)

| Reaction Time (min) | Desorption Outgassing Temperature (°C) 600 | | 700 | | 950* | |
|---|---|---|---|---|---|---|
| | θ | ΔH | θ | ΔH | θ | ΔH |
| 2 | 0.68 | 75 | 0.64 | 81 | 0.46 | 80 |
| 4 | 0.69 | 75 | 0.66 | 81 | 0.48 | 78 |
| 6 | 0.70 | 74 | 0.68 | 79 | 0.49 | 77 |
| 8 | 0.71 | 73 | 0.69 | 76 | 0.50 | 76 |
| 10 | 0.71 | 73 | 0.70 | 74 | 0.51 | 77 |
| 12 | 0.72 | 72 | 0.71 | 73 | 0.52 | 78 |
| 15 | 0.72 | 72 | 0.71 | 76 | 0.53 | 78 |
| 20 | 0.73 | 72 | 0.72 | 78 | 0.54 | 76 |
| 25 | 0.74 | 72 | 0.73 | 76 | 0.55 | 77 |
| 28 | 0.75 | 72 | 0.74 | 76 | 0.56 | 76 |
| $(\Delta H)_{Av}$ | 73 ± 2 | | 77 ± 4 | | 76 ± 4 | |

*Followed by 600°C desorption temperature

Table 9. Dependence of ΔH (kcal/mole) at 100°C on Surface Coverage (θ) (Desorption Temperatures = 450, 500, and 550°C)

| Reaction Time (min) | Desorption Temperature (°C) 450 | | 500 | | 550 | |
|---|---|---|---|---|---|---|
| | θ | ΔH | θ | ΔH | θ | ΔH |
| 2 | 0.81 | 58 | 0.72 | 52 | 0.70 | 64 |
| 4 | 0.82 | 55 | 0.73 | 53 | 0.71 | 64 |
| 6 | 0.82 | 56 | 0.74 | 54 | 0.72 | 63 |
| 8 | 0.83 | 57 | 0.75 | 55 | 0.72 | 64 |
| 10 | 0.83 | 56 | 0.75 | 55 | 0.73 | 63 |
| 12 | 0.84 | 57 | 0.76 | 55 | 0.74 | 64 |
| 15 | 0.84 | 59 | 0.76 | 56 | 0.74 | 64 |
| 20 | 9.85 | 58 | 0.77 | 57 | 0.75 | 64 |
| 25 | 0.86 | 59 | 0.78 | 58 | 0.76 | 64 |
| 28 | 0.86 | 58 | 0.78 | 58 | 0.77 | 63 |
| $(\Delta H)_{Av}$ | 57 ± 2 | | 55 ± 3 | | 64 ± 1 | |

again subjected to the same heat treatment procedure, that is, heat treatment up to the desired desorption temperature. A second adsorption run at 100°C was then made. The adsorption-desorption cycle was once more repeated on the same sample after which a third adsorption run was made. Values of $\theta$ and $\Delta H$ for the three cycles are given in Table 10 for desorption temperatures of 500, 600, and 700°C. For a desorption temperature of 500°C, $\Delta H$ for the three cycles is almost constant and amounts to 54 ± 1 kcal/mole. This is true for values of $\theta$ between 0.72 and 0.90. For desorption temperatures of 600 and 700°C, the average value of $\Delta H$ for each cycle, $(\Delta H)_{Av}$, is independent of $\theta$ within the limits of the cycle. However, there exists a sudden drop in $(\Delta H)_{Av}$ for each successive cycle. Apparently, heat treatment of the surface completely covered by chemisorption oxygen may regenerate a surface having sites different than those in the case of a fresh sample where its original surface is partially covered with oxygen. Thus, $\Delta H$ seems to be dependent on the history of the sample. This hypothetical assumption is valid for desorption temperatures 600 and 700°C.

Table 10. Variation of $\Delta H$ (kcal/mole) at 100°C with Surface Coverage ($\theta$) for Recycled Samples

| Desorption Temperature (°C) | Cycle 1 | | Cycle 2 | | Cycle 3 | |
|---|---|---|---|---|---|---|
| | $\theta_1$ | $(\Delta H)_{Av}$ | $\theta_2$ | $(\Delta H)_{Av}$ | $\theta_3$ | $(\Delta H)_{Av}$ |
| 500 | 0.72 - 0.78 | 55 ± 3 | 0.79 - 0.84 | 55 ± 3 | 0.87 - 0.90 | 53 ± 3 |
| 600 | 0.68 - 0.75 | 73 ± 2 | 0.73 - 0.80 | 62 ± 3 | 0.82 - 0.87 | 55 ± 2 |
| 700 | 0.64 - 0.74 | 77 ± 4 | 0.68 - 0.77 | 49 ± 3 | 0.71 - 0.77 | 40 ± 4 |

At this stage, progress of experimental work done by both DSC and TGA techniques has, so far, thrown enough light towards understanding the nature of the oxygen chemisorption process on a relatively clean carbon surface, this is Saran. Therefore, it is time to apply and thus extend some of those previously reported findings on Saran to the case of other carbonaceous materials, for example coals and chars. Further exploratory experimental work must be done before an exact forecast can be made.

FACET V-A: COMBUSTION OF CHARS AND LOW VOLATILE FUELS

## COMBUSTION OF CHAR AND ANTHRACITE COAL IN LARGE UTILITY BOILERS (TASK 33)

### Introduction

The theoretical aspects of the study of combustion of low volatile fuels have been resumed and now focus on the computer model of a plane flame furnace firing low volatile fuels, and expanding it to account for heat losses through the furnace walls.

The development of a one-dimensional model to analyze and explain past experiments has been presented in previous quarterly reports. Now including heat losses through the side walls, the model considers the balance of energy as expressed by the equation

$$\bar{\rho}_o v_o \bar{C} dT/dz = \dot{Q}_{rel} + \dot{Q}_{rad} - \dot{Q}_{loss} \tag{9}$$

where $\bar{\rho} = \rho_o + D_o$ is an equivalent dust cloud density and $v_o$ is the inlet mixture velocity, both at ambient conditions. $\bar{\rho}_o$ and $D_o$ are the air density and dust cloud density (g/cm$^3$), respectively, also at ambient conditions. $\bar{C}$ is an equivalent specific heat for the mixture (cal/g°C), and T is the mixture temperature at a point z from the left wall. $\dot{Q}_{rel}$ is the rate at which heat is released per unit volume due to fuel combustion; $\dot{Q}_{rad}$ is the net rate at which radiant energy is absorbed per unit volume; and $\dot{Q}_{loss}$ is the net rate at which heat is lost by radiation to the side walls. For a steady state this loss to the side walls is equal to the heat conducted through the walls.

The heat release rate $\dot{Q}_{rel}$ is given by

$$\dot{Q}_{rel} = 4\pi r^2 N_{v,o} R_s q \, T_o/T \tag{10}$$

where q is the calorific value of the fuel; $N_{v,o}$ is the number of monosized particles of radii r per unit volume; and $R_s = P_g K_c K_d/(K_d + K_c)$ is the surface specific reaction rate (g/cm$^2$sec) for a solid particle. $P_g$ is the ambient oxygen partial pressure; $K_c$ and $K_d$ are the chemical and diffusional reaction rate coefficients (g/cm$^2$ s atm), respectively.

The net rate of radiative absorption can be expressed as

$$\dot{Q}_{ral} = -4\sigma k T^4 + 2\sigma k T_{w1}{}^4 E_2(\tau) + 2\sigma k T_{w2}{}^4 E_2(\tau - \tau) + 2\sigma k \int_0^{\tau} L\, T^4(t)\, E_1(|\tau - \tau|)\, dt \qquad (11)$$

where $\sigma$ is the Stefan-Boltzman constant; k is the mixture absorption coefficient; $T_{w1}$ and $T_{w2}$ are the "left" and "right" wall temperatures; and $\tau$ and $\tau_L$ are the optical depths of the points at the distances z and L from the "left" wall. The functions $E_1$ and $E_2$ are the first and second exponential integrals, where the nth exponential integral is defined by $E_n(t) = \int_0^1 \mu^{n-2} e^{-t/\mu} d\mu$, and where $E_n(t)kt = -E_{n+1}(t)$ was used to obtain the equation (11). The four terms on the right-hand side of equation (11) are the rate at which an element radiates to its surroundings, and the rate at which it absorbs energy from the "left" or inlet wall, from the "right" or outlet wall, and from the rest of the mixture, respectively. Solution of the boundary value problem neglecting the radiation losses to the side walls has yielded temperature profiles illustrated in Figure 21. They are characterized by steeper temperature profiles and higher peak temperatures than experimentally observed (Figure 22) by Howard and Essenhigh[9] for coal, especially for the higher reactivities (those approaching the Field[10] values).

The inclusion of radiation losses to the side walls was introduced to determine their effect on these temperatures. Estimates of these losses were made by assuming boundary (wall) temperatures, and radiation rate expressions in order to obtain a reasonable approximation to the distribution of radiation losses to the side walls. A simple first try considered the net rate of energy loss by radiation to the furnace walls given by

$$\dot{Q}_{loss} = U_1 (T_g - T_{abm})$$

where $U_1$ is a conduction heat transfer coefficient, $T_g$ is the gas temperature, and $T_{amb}$ = 21°C is the ambient temperature. For the same particle density considered previously, and for $\beta$ = 0.75 (0.75 X standard Field reactivity), the temperature profile was less satisfactory then before (Figure ) where wall losses were not considered. A second try considered

$$\dot{Q}_{loss} = U_2 \sigma T_g{}^3 (T_g - T_{amb})$$

and again produced unrealistically high peak temperatures.

The most recent representation (Figures 21 and 22) of net rate of radiation loss to the walls was

$$Q_{loss} = U_3 \sigma (T^4{}_g - T^4{}_{avg})$$

where $T_{avg}$ is an assumed average wall temperature (≃ 950°C). The constant $T_{avg}$ applied in this model is based on experiments with the plane flame furnace, and reduces the complexity of the view factor and gas radiative interchange

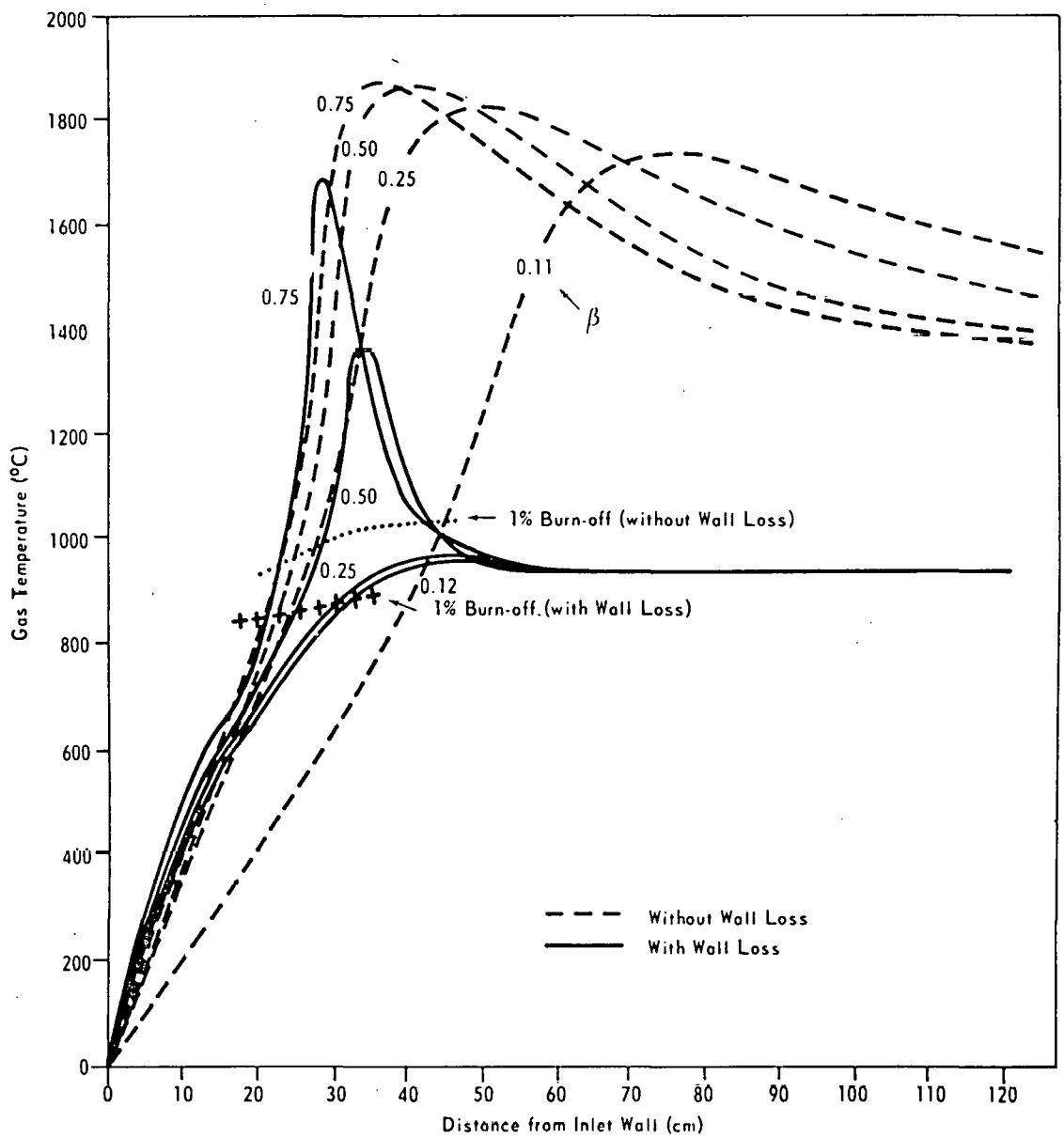


Figure 21. EFFECT OF REACTIVITY MULTIPLIER ($\beta$) ON GAS TEMPERATURE PROFILE

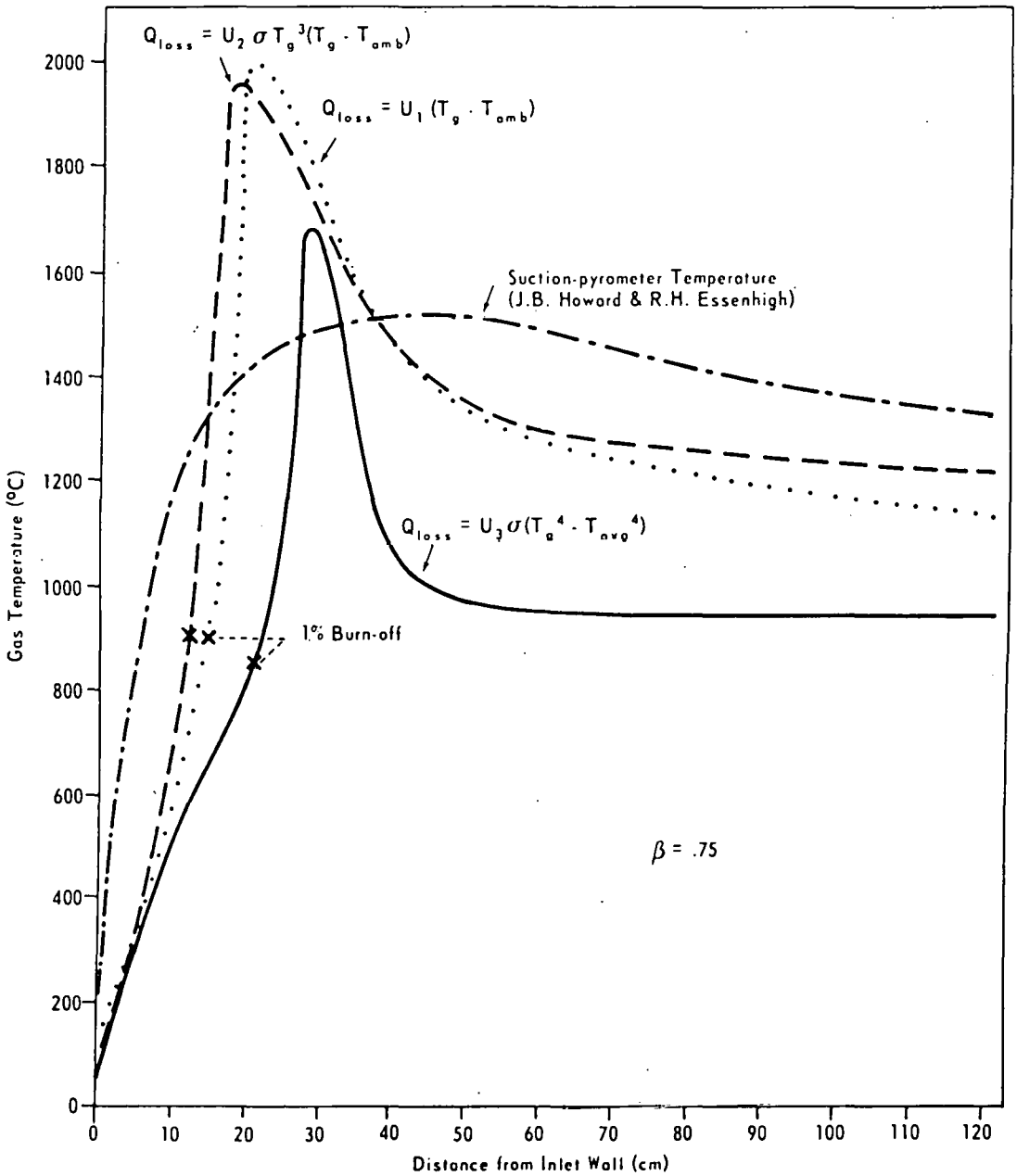


Figure 22. TEMPERATURE PROFILES VS DISTANCE FROM INLET WALL FOR DIFFERENT $Q_{loss}$

computations. A one percent burn-off was arbitrarily adopted as an index for the location of the flame front. The results indicate a great sensitivity of the peak flame temperatures to the reactivity parameter, but they are unrepresentative of the experimentally measured temperatures and profiles.

Continued efforts will be directed toward obtaining a set of reaction rate and radiation equations which provide temperature profiles adequately representing the real system.

## FACET V-B: COMBUSTION OF COAL-OIL EMULSIONS

### COMBUSTION OF COAL-OIL-WATER-AIR MIXTURES (TASK 34)

The importance of complete characterization of the hot-wall laboratory furnace with which this research is being conducted has become increasingly evident during the last several quarters. The last quarter's report introduced a concerted attack on this problem in order that the data collected in the past and future can be properly evaluated and analyzed. This work continued during the past quarter with the summer services of Dr. Karl Lockwood, Professor of Chemistry at Lebanon Valley College. From a sequence of 4 furnace runs firing #2 fuel oil, smoke points were determined be extrapolation as illustrated in Figure 23. The percent obscuration recorded from the installed smoke meter has been plotted against the secondary air flow rate (scfm). The smoke point defined by linear extrapolation to the zero smoke level from the low excess air region was reproducible if certain precautions were observed. Most important, the smoke meter lenses were, and must be cleaned between all excursions into smoke regions. On 3 other runs, at low firing rate, a balanced draft could not be maintained sufficiently below smoke point to permit an extrapolation. Hence, a lower limit on firing rate (about 900,000 Btu/hr) was established below which an unbalanced draft denies control of combustion 100 percent consistent with our research objectives.

A very informative set of experiments was conducted to relate furnace efficiency to the thermal state of the furnace. Short of thermal equilibrium, the repeatability of experimental data is unlikely if the firing and thermal load histories are not equivalent. And yet a requirement that all furnace data be acquired from conditions of furnace equilibrium is impractical from a consideration of time and cost. Therefore, simple correlations between efficiency, firing history, and load history must be established in order to evaluate and compare non-equilibrium experiments. The dynamics of the furnace and combustion process can also be used to separate radiation and conduction mechanisms of heat transfer, permitting more complete evaluation of the phenomena most important to us--the combustion characteristics of the various fuels themselves.

Figure 24 illustrates one of a number of runs from which percent furnace efficiency determined from the heat transfer to the seventeen water tubes at the furnace floor has been plotted against time of firing at a constant rate after light-off. Since one set of water tube and firing data takes almost an hour to record, the efficiency plotted at each time is a time-averaged measure. Hence the first determination of furnace efficiency is for a time beyond light-off of at least 1/2 hour. Extrapolation back to the zero time intercept provides an estimate of the amount of radiation heat transfer to the water tubes attributable to the flame itself--that heat flux present immediately upon furnace light-off. This value is about 1/3 of the asymptotic equilibrium value which is due to increasing contributions of radiation from the walls of increasing temperature. Taking data from several tubes only, a similar evaluation of the transition from fired to unfired conditions

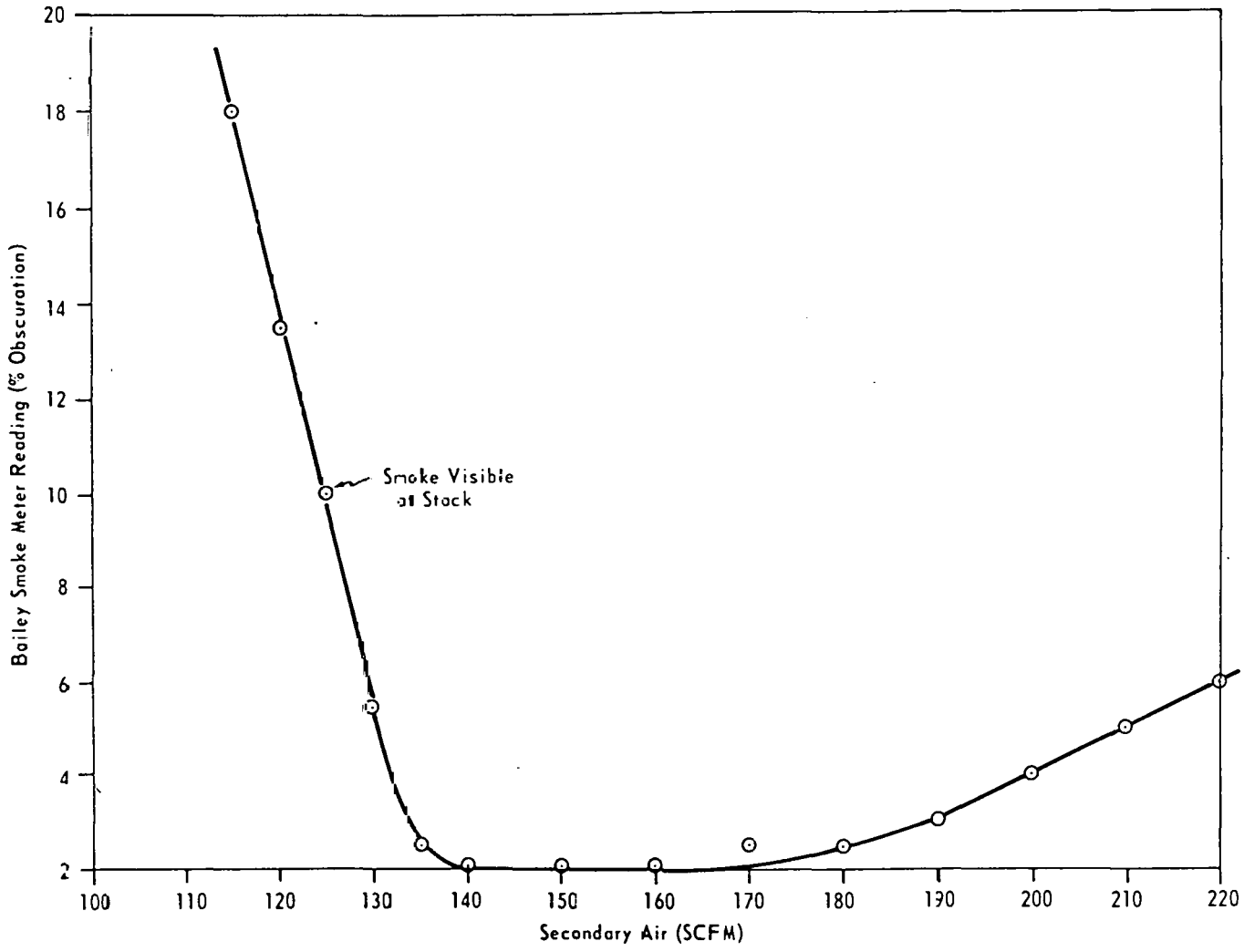


Figure 23. SMOKE FORMATION AS A FUNCTION OF SECONDARY AIR FLOW Run #21 = 8/9/77
0.0170 Rotameter Firing Rate = 7.05 gal/hr = 0.939 x $10^6$ Btu/hr

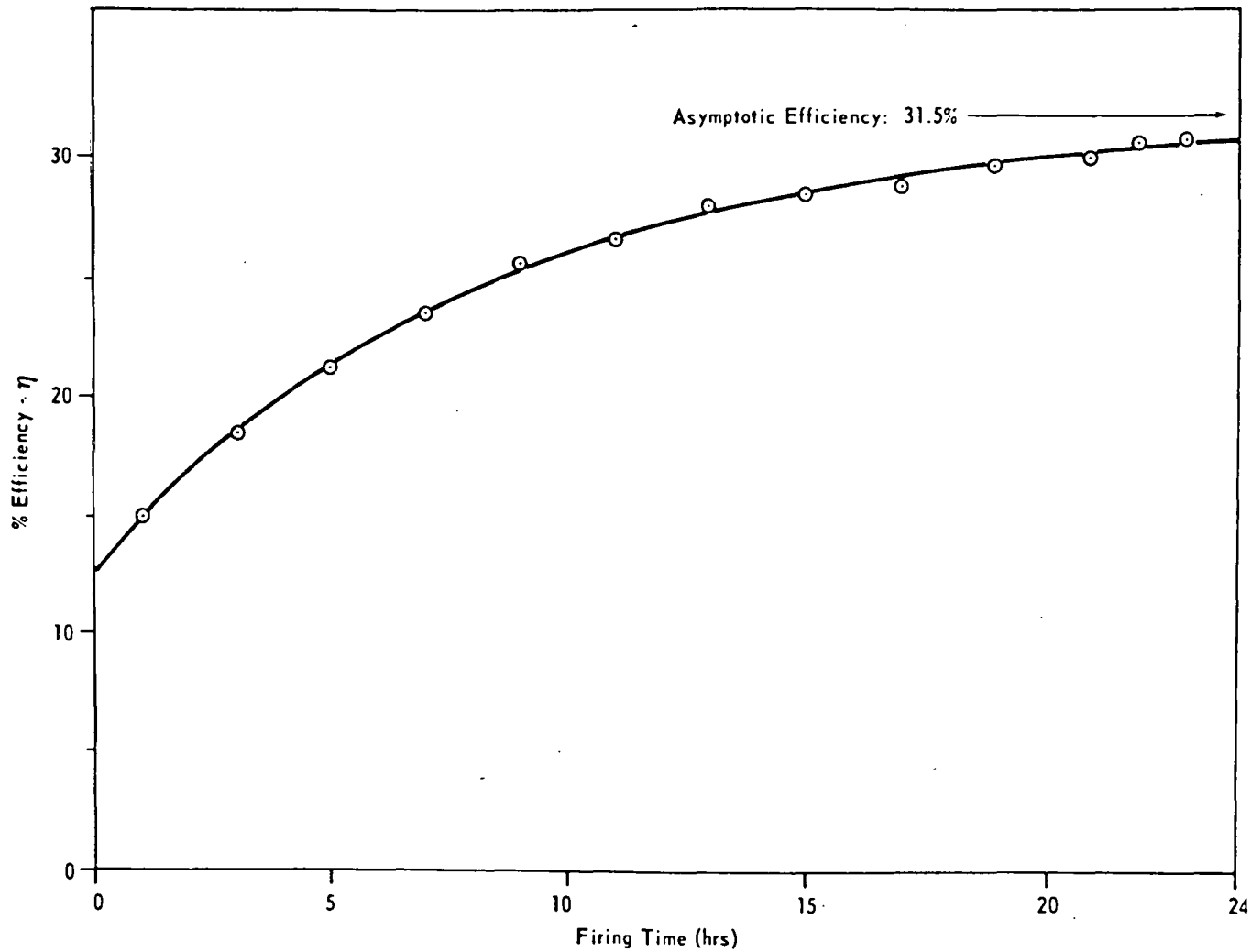


Figure 24. PERCENT EFFICIENCY VERSUS ELAPSED FIRING TIME Run #1 = 5/31/77
Firing Rate (#2 oil) = 8.02 gal/hr = $1.07 \times 10^6$ Btu/hr = $2.69 \times 10^5$ kcal/hr

revealed an instantaneous drop in heat transfer rate corresponding to the instantaneous elimination of the flame radiation, leaving the decreasing contribution of the cooling walls. That the equilibrium value of efficiency is approached exponentially is verified by Figure 25, in which the slope of a linear relation between log $(\eta_\infty - \eta)$ and firing time is related to the characteristic time of the furnace. Such curves as these will be more easily obtained once a computerized data acquisition scheme is incorporated into the experimental set-up, hopefully within the next quarter.

Examination of past tube efficiency profiles has suggested that the lack of furnace symmetry and dimensional uniformity may be a source of trouble in evaluating data. For instance, water tubes located near the large observation port normally closed by a sliding door had noticeably different efficiencies. Bricking in the recess of the wall at this sliding door to make the wall uniform revealed that the nearby tubes had received less wall radiation because of the recess. This deficiency is now considered remedied.

At about the same time it became evident that the insertion and removal of water-cooled radiation probes also influences the heat transfer and furnace efficiency calculations. The heat transferred to these water-cooled probes contributes about 5 percent to the total furnace efficiency of 30 percent when included in the efficiency calculations. In other words, from 16 to 20 percent of the heat transferred to the load is received by these radiation measurement probes which receive radiation from 360° of viewing angle within the flame itself.

Numerical modeling of the heat flux and temperature profiles through the furnace walls continued to be developed during this quarter, with reasonable agreement obtained with experimental measurements. The successful completion of this modeling effort will permit a more reliable evaluation of the heat balance of the furnace to be obtained.

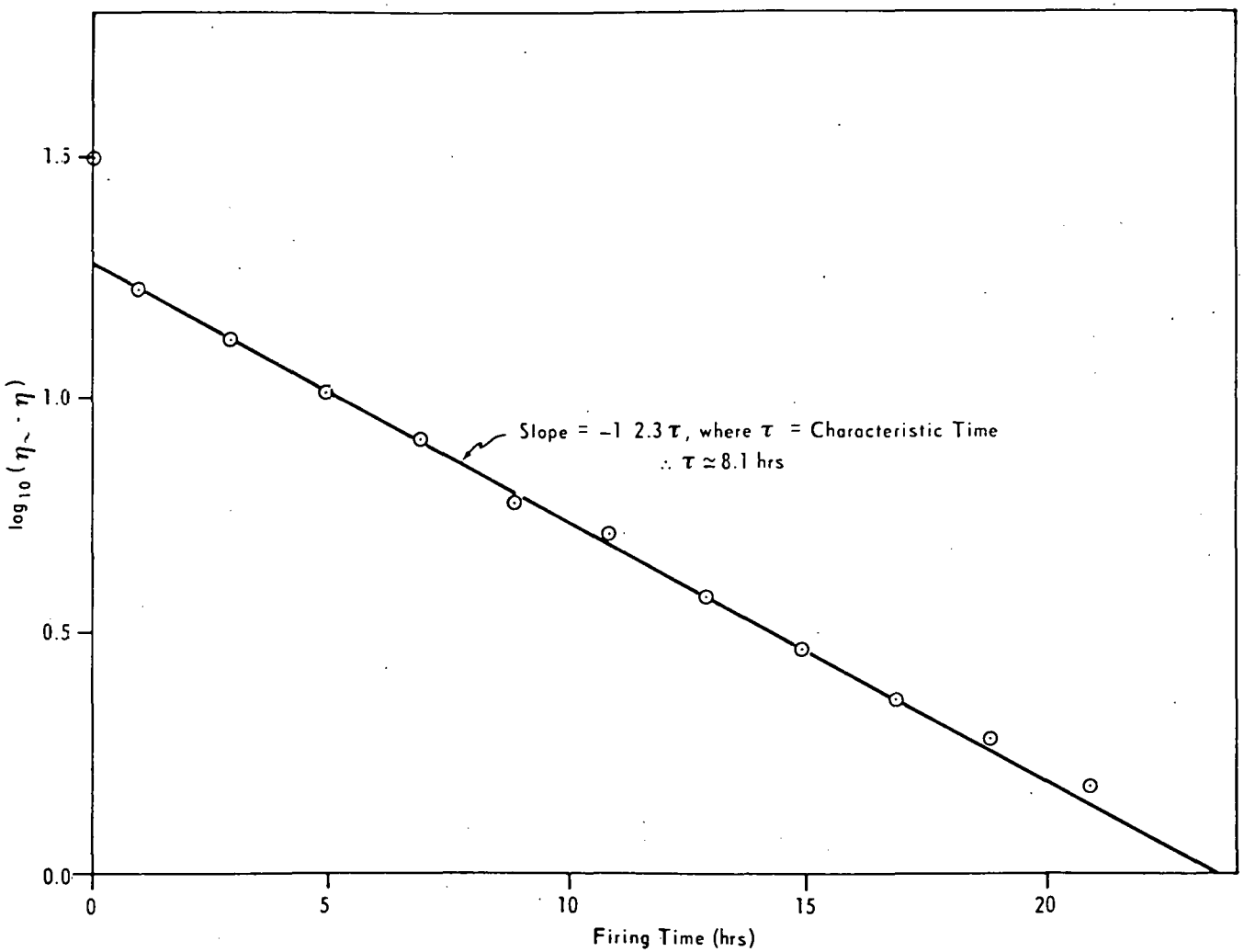


Figure 25. $LOG_{10}(\eta_\infty - \eta)$ VS FIRING TIME Run #1 = 5/31/77

# CONCLUSIONS

## FACET I-D: PENN STATE/ERDA COAL DATA BASE

### Task 17: Structuring and Utilization of the Data Base

A statistical analysis of 119 coal channel samples selected from the Penn State/ERDA coal data base is complete. Factor and cluster analyses of selected chemical and petrographic properties show that these coals can be dissected into four groups distinguished on the basis of coal rank, relative maceral composition, and organic sulfur content. Factor analyses of these individual groups provide insight into the various stages of coalification. In the future, these four groups, determined by cluster analysis, may be useful in the selection of representative coal types for the study of coal behavior during industrial use.

## FACET IV-A: REACTOR DEVELOPMENT AND OPERATION

From combustion pot experiments on two different cokes it is apparent that the values of activation energy for the carbon/carbon dioxide reaction in a non-diffusional system, and the reaction rate constant, $n_1$, for the combustion region are essentially independent of coke type. The data on gasification reactions within a coke bed provide an important base for the development of a numerical model, and the evaluation of coals.

## FACET IV-B: COKES AND CHARS

### Task 27: Effect of Variables on Char Structures

By use of a TGA apparatus the weight changes which are associated with preoxidation can be followed reproducibly. The amount of oxygen chemisorbed is a function of both temperature and particle size. For particles of PSOC-337 (a Pennsylvania high volatile A coal) in the range 200 x 250 mesh significant gasification takes place at 200°C as well as oxygen chemisorption.

Water densities of 19 coals, determined at 25°C in the presence of a wetting agent, were invariably lower than those water densities measured in the absence of the wetting agent. The densities in the presence of the wetting agent are lower than the corresponding helium densities for coals varying in rank from anthracite to medium volatile bituminous; for lower rank coals the helium densities are invariably lower.

### Task 30: Effect of Catalytic Cations on Gasification

Study of the effect of reaction temperature on gasification of Saran carbon in air shows one percent platinum loading on Saran carbon increases.

gasification rates over the entire range of carbon burn-off. Reactivity of Saran carbon is independent of particle size at a reaction temperature of 500°C.

## FACET IV-F: DIFFERENTIAL SCANNING CALORIMETRY

### Task 31: DSC in Evaluation Coals for Conversion

For the air-activated Saran carbon (activated to 63.8% carbon burn-off) the value of $\Delta H$ (kcal/mole) for oxygen chemisorption at 100°C is independent of surface coverage $\theta$ (where $0.46 < \theta < 0.75$). For desorption temperatures of 600, 700, and 950°C prior to oxygen chemisorption at 100°C, the values of $\theta$ vary between 0.46 and 0.75; however, the average value of $\Delta H$, $(\Delta H)_{Av}$ is almost constant and amounts to 74 ± 3 kcal/mole. For desorption temperatures of 450, 500, 550, and 600°C, the values of $(\Delta H)_{Av}$ are: 57 ± 2, 55 ± 3, 64 ± 1, and 74 ± 3 kcal/mole, respectively. Thus, increase in desorption temperature from 450 to 600°C prior to oxygen chemisorption at 100°C increases the value of $(\Delta H)_{Av}$. Subjecting the surface to successive absorption-desorption cycles indicates that a given value of $\Delta H$ is basically dependent on the history of the sample. This is only valid when the temperature of the desorption cycle is 600°C or higher.

## FACET V-A: COMBUSTION OF CHARS AND LOW VOLATILE FUELS

Attempting to bring the results of computer modeling into closer agreement with the experimental data from the plane flame furnace, crude representations of radiation losses to the furnace walls were introduced. A small number of schemes were used whereby this radiation loss was accommodated as a continuously distributed heat sink in the ideal plane flame model. The resulting distortion of profiles, producing sharp flame temperature peaks, is an indication that more representation reaction rate and radiation equations must be considered.

## FACET V-B: COMBUSTION OF COAL-OIL EMULSIONS

### Task 34: Combustion of Coal-Oil Emulsions

A digression from the main objectives of the research has been essentially completed, having provided a much improved understanding of the experimental furnace, and a characterization of its equilibrium behavior and dynamic responses. This work has led to minor furnace and control modifications, improvements in operating procedures, and an improved basis for evaluating experimental data toward accomplishment of the major objectives: the investigation of the combustion characteristics of coal-oil-water-air fuel mixtures.

Only through the use of non-equilibrium experiments can certain important combustion characteristics be studied, and computerized data acquisition

is being developed to fully implement such methods. Specifically, the determination of the furnace characteristic time ($\sim$ 8 hrs) is sufficient to permit the comparison of the behavior of various fuels without actually attaining equilibrium. Non-equilibrium experiments also permit the distinction between the heat transferred by radiation from the flame to the water tubes, and that received from the hot furnace walls.

## REFERENCES


1. Kobayashi, H., J.B. Howard, and A.F. Sarofim. Coal Devolatilization at High Temperatures. Proc. Sixteenth Symposium XX (International) on Combustion, The Combustion Institute, p. 411, 1976.

2. Spackman, W., A. Davis, P.L. Walker, H.L. Lovell, R.H. Essenhigh, F.J. Vastola, and P.H. Given. The Characteristics of American Coals in Relation to Their Conversion into Clean Energy Fuels. Qtr. Tech. Prog. Rept. from The Pennsylvania State University to ERDA, 185 pp., Jan.-Mar. 1977.

3. Nsakala, N., R.H. Essenhigh, and P.L. Walker, Jr. Studies on Coal Reactivity: Kinetics of Lignite Pyrolysis in Nitrogen at 808°C. Combustion Science Technology, (in press).

4. Spackman, W., A. Davis, P.L. Walker, H.L. Lovell, R.H. Essenhigh, F.J. Vastola, and P.H. Given. The Characteristics of American Coals in Relation to Their Conversion into Clean Energy Fuels. Qtr. Tech. Prog. Rept. from The Pennsylvania State University to ERDA, 34 pp., Apr.-June 1977.

5. Nsakala, N., R.H. Essenhigh, and P.L. Walker, Jr. The Characteristics of Chars Produced by Pyrolysis Following Rapid Heating of Pulverized Coal. Tech. Rept. 2 from The Pennsylvania State University to ERDA, 162 pp., 1977.

6. Badzioch, S., and P.G.W. Hawksley. Kinetics of Thermal Decomposition of Pulverized Coal Particles. Ind. Eng. Chem. Process Des. Devel., v. 9, p. 521, 1970.

7. Eapen, T.R. Blackadar, and R.H. Essenhigh. Proc. Sixteenth Symposium (International) on Combustion, The Combustion Institute, p. 515, 1976.

8. Ettinger, I.L., and E. Zhupakhina. Method of Determining Porosity or Mineral Coals. Fuel, v. 39, p. 387, 1960.

9. Howard, J.B., and R.H. Essenhigh. Mechanism of Solid-Particle Combustion with Simultaneous Gas-phase Volatiles Combustion. Proc. Eleventh Symposium (International) on Combustion, The Combustion Institute, p. 399, 1967.

10. Field, M.A. Rate of Combustion of Size-graded Fractions of Char from a Low Rank Coal Between 1200°K and 2000°K. Combustion and Flame, v. 13, p. 273, 1969.

The following persons have made contributions to this report: J.C. Cogoli, C.P. Dolsen, T. Eapen, H. Gong, D.S. Hoover, J.M. Hower, I.K. Ismail, R.G. Jenkins, K.W. Kuehn, K.L. Lockwood, O.P. Mahajan, D. Maloney, N. Nsakala, H.E. Shull, R. Taylor, and D. Xieu.



*U.S. GOVERNMENT PRINTING OFFICE: 1978-740-306/9563. Region 4.